

Review

Recent Advances in Real-Time Pluvial Flash Flood Forecasting

Andre D. L. Zanchetta ^{1,*}  and Paulin Coulibaly ^{1,2,3}

¹ Department of Civil Engineering, McMaster University, 1280 Main Street West, Hamilton, ON L8S 4L7, Canada; couliba@mcmaster.ca

² School of Geography and Earth Sciences, McMaster University, 1280 Main Street West, Hamilton, ON L8S 4L7, Canada

³ United Nations University Institute for Water, Environment, and Health, Hamilton, ON L8P 0A1, Canada

* Correspondence: dellalia@mcmaster.ca

Received: 29 January 2020; Accepted: 15 February 2020; Published: 19 February 2020



Abstract: Recent years have witnessed considerable developments in multiple fields with the potential to enhance our capability of forecasting pluvial flash floods, one of the most costly environmental hazards in terms of both property damage and loss of life. This work provides a summary and description of recent advances related to insights on atmospheric conditions that precede extreme rainfall events, to the development of monitoring systems of relevant hydrometeorological parameters, and to the operational adoption of weather and hydrological models towards the prediction of flash floods. With the exponential increase of available data and computational power, most of the efforts are being directed towards the improvement of multi-source data blending and assimilation techniques, as well as assembling approaches for uncertainty estimation. For urban environments, in which the need for high-resolution simulations demands computationally expensive systems, query-based approaches have been explored for the timely retrieval of pre-simulated flood inundation forecasts. Within the concept of the Internet of Things, the extensive deployment of low-cost sensors opens opportunities from the perspective of denser monitoring capabilities. However, different environmental conditions and uneven distribution of data and resources usually leads to the adoption of site-specific solutions for flash flood forecasting in the context of early warning systems.

Keywords: flash flood; flood forecast; flood prediction; rainfall prediction; precipitation forecast; early warning systems; flood inundation forecast

1. Introduction

Flash floods (FFs) are among the most damaging types of weather-related disasters faced nowadays. They may be caused either by extreme precipitation, by the failure of human-made structures, such as dams, or by complex water-snow interactions. The fast development of FFs imposes additional challenges for early prediction when compared to riverine floods. Structural measures adopted to reduce the impact of these events include the construction of physical components aimed to enhance the overall resilience of drainage systems, such as levees and detention ponds. Nonstructural solutions include the adoption of regulations for land use/occupation, personal training for responsive actions, and the implementation of operational flash flood early warning systems (FFEWSs).

A core feature of FFEWSs is the capability to perform timely and accurate FF forecasts. Methods for FF forecasting demand continuous improvement, mainly in the current context of progressive changes in urbanization and climate patterns that lead to an increased susceptibility to FFs observed in different locations worldwide [1–3]. The work developed by Hapuarachchi et al. in 2011 [4] brings comprehensive state-of-the-art for its time in the topics of input data, modeling approaches and

estimation of uncertainties related to FF forecasting. Since then, several advances were observed in multiple related fields driven by an expansion of monitoring capabilities, consolidation of extensive datasets, and the establishment of higher resolution models due to increasing computational power.

The objective of this review paper is to provide a centralized summary of recent developments associated with FF forecasting with a focus on existing or potential real-time operational applications and to discuss the latest insights on promising opportunities for their enhancement. The main contribution of this paper relies on answering the questions, “How has flash flood forecasting evolved in the last decade?” and “Which are the current major gaps and trends in this field?”.

As such, a non-structured literature review was performed over a selected number of papers published in renowned peer-reviewed journals, official technical reports, and conference abstracts considered relevant for topics related to the enhancement of operational FF forecasting.

Scope, Definitions, and Work Structure

Flash floods are defined by the United States’ (US) National Weather Service as “A rapid and extreme flow of high water into a normally dry area, or a rapid water level rise in a stream or creek above a predetermined flood level, beginning within six hours of the causative event (e.g., intense rainfall, dam failure, ice jam)” [5]. From an operational perspective, priority is usually given to the capability of predicting their occurrence, while for riverine floods primary importance is given to the prediction of their magnitudes [6].

Various terminologies can be applied for specific activities associated with prediction systems. In this work, “anticipation” is used to qualitatively describe the expected occurrence/non-occurrence of an event in the near future, with no (or very few) details about the upcoming scenario. The term “forecast” is used for the activities that generate quantitative information in time and space. Specifically, the terms “short-term forecast” and “nowcast” are used for forecast windows of up to 6 h [7,8], and “long-term forecast” is applied when the forecast window is longer.

This work considers only events driven by extreme precipitation due to their significantly higher occurrence when compared to the ones triggered by other circumstances. Pluvial FFs can be caused by deep and local convective precipitation, orographic effects, storm surges, and cyclones. As cyclones are usually associated with synoptic-scale patterns and have their specific and extensive research field, they are not explicitly discussed in this work. From this perspective, FF forecasting is highly related to the challenging meteorological problem of predicting extreme local rainfall events [9].

Multiple approaches were proposed and implemented for FF prediction as environments with different configurations and available datasets are prone to such types of hazards, usually leading to the adoption of customized solutions. FF prone areas include non-urban steep catchments [10], urban or semi-urban catchments [2], urban neighborhoods served [11] (or not [12]) by a central drainage channel, and coastal urban zones [13], as illustrated in Figure 1. In this work, we use the expression “catchment” (and “sub-catchment”) for areas in which runoff is directed to a single outlet point (and an inlet point is present). When the boundaries of the study area take into consideration non-geomorphological delineations (as administrative borders), the term “neighborhood” is used. When both boundary definitions are acceptable, the expressions “zone” or “environment” are interchangeably used.

As this type of hazard is mainly characterized by occurring with short development time and on small catchments, advances towards: (1) increase in the spatiotemporal resolution and precision of input and output data, (2) increase of overall lead time and awareness, and (3) reduction of the total computational expenses for the generation of relevant products are assumed to be of interest to the problem and are explored in this work.

The discussion is presented as follows. In Section 2, the different approaches usually adopted to determine whether a FF is expected or not are described. In Section 3, we comment on results from a selected number of recently published exploratory analyses on atmospheric contributing factors for extreme precipitation events. In Section 4, recent advances and developments on remote sensing techniques relevant to the subject are commented on. Precipitation prediction and hydrodynamic

models involved in forecasting chains are presented in Sections 5 and 6, respectively. The work is concluded with a summarizing discussion of the key findings from the presented literature review and recommendations of future work in the field.

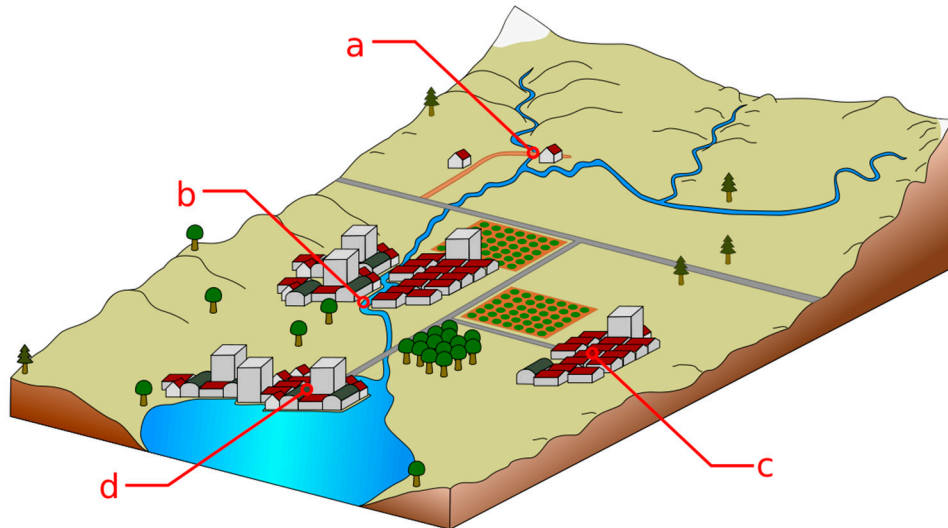


Figure 1. Different types of flash flood-prone environments include (a) non-urban steep catchments and (b) urban neighborhoods served or (c) not by a central drainage channel, and (d) coastal urban zones.

2. Criteria for Deciding Flash Flood Occurrence

At the operational time, the resolution of whether or not a FF event is expected to happen in the near future at a given location can be determined through different approaches and it is usually responsible for triggering (or not) the first responsive actions to the upcoming hazard. The choice of which method to adopt depends on multiple factors, including resource availability, previous experience acquired, and even personal preferences of the operational team. The different approaches are presented in four classes (Section 2.1 to 2.4), sorted by an increasing level of complexity. Such division is derived from the classification adopted by Hapuarachchi et al. [4], with the difference that two families of rainfall comparison methods are defined, taking into consideration whether surface conditions are considered or not in the representation of the rainfall-runoff process. A simplified diagram of the different families of approaches is presented in Figure 2.

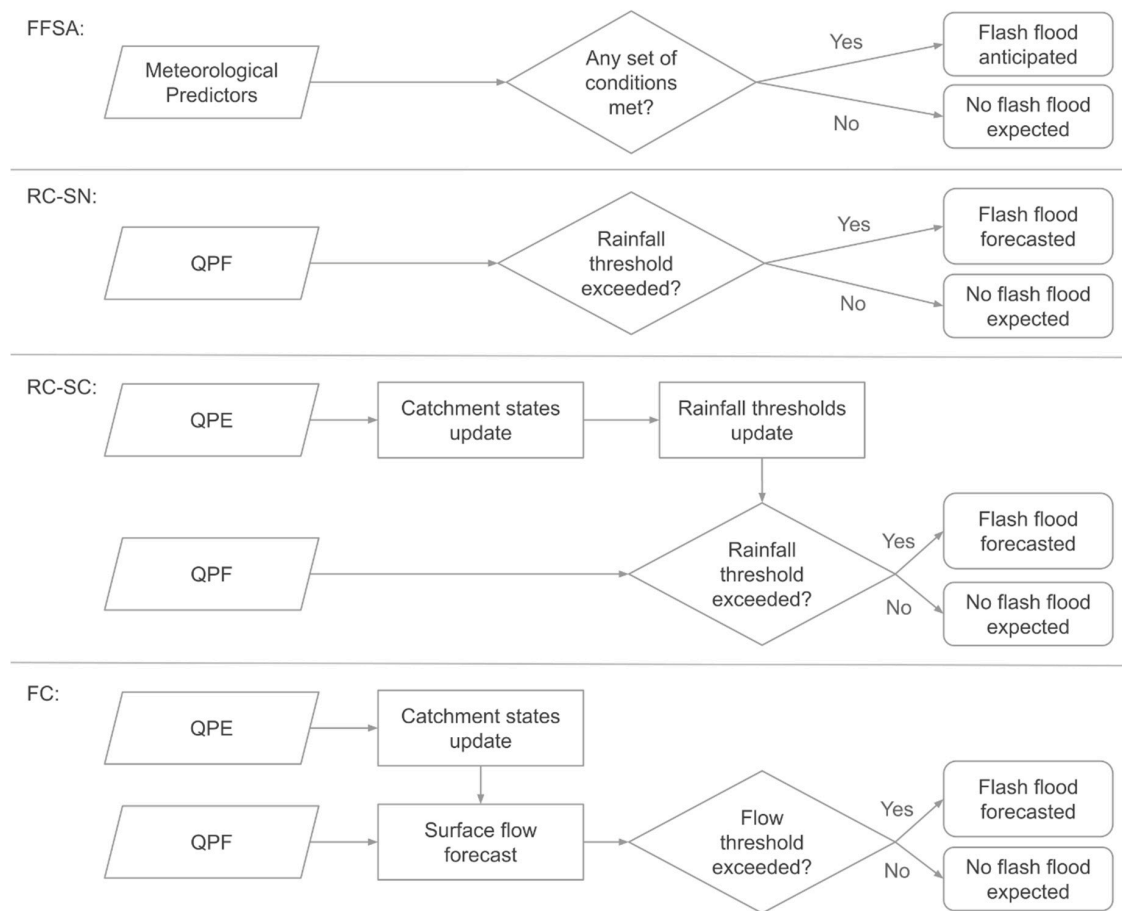


Figure 2. Overall workflows adopted by the different decision approaches usually present in flash flood early warning systems (FFEWS). FFSA, flash flood susceptibility assessment; RC-SN, rainfall comparison with surface conditions neglected; RC-SC, rainfall comparisons with surface conditions considered; FC, flow comparison; QPF, quantitative precipitation forecast; QPE, quantitative precipitation estimations.

2.1. Flash Flood Susceptibility Assessment (FFSA)

One relatively simple approach that can be used as a first step for anticipating FF events is based on the assessment of multiple hydrometeorological conditions known to precede extreme precipitation scenarios. It can be performed through ingredients-based [14], checklists [15], or scoring techniques [16].

Quantitative precipitation forecast (QPF) products are frequently considered to be part of the data available for FF forecasters. However, when they are missing or considered not reliable, a core objective becomes the prediction of extreme rainfall events itself. Meteorological parameters traditionally explored for such include precipitable water (PW), relative humidity (RH), dew point temperature (T_d), convective available potential energy (CAPE), and the so-called K-index, which describes the local potential for thunderstorms [17]. When antecedent surface conditions, such as surface soil moisture (SSM), are part of the predictors, they are accounted for through simplified means, such as the integration of recently observed precipitation. Due to its meteorological-driven basis, this family of monitoring activities is usually performed by weather service teams (i.e., meteorologists) instead of by river forecast centers (i.e., hydrologists).

Research areas of benefit for the flash flood susceptibility assessment (FFSA) include the search for optimal meteorological FF predictors, the application of data provided by newly available meteorological monitoring systems by operational teams, and the proposal of strategies to communicate uncertainties associated with the eventual unavailability of part of the data used [18].

2.2. Rainfall Comparison with Surface Conditions Neglected (RC-SN)

When QPF products are available, the decision of whether a FF is expected to happen on a catchment can be made based solely on a threshold-exceedance assessment of the predicted peak precipitation accumulation value [19].

Rainfall frequency analysis approaches can be used for establishing the raw static thresholds. Rainfall return periods are usually adopted on FFEWS designed for large areas covering multiple low-urbanized catchments, since such locations are usually poorly monitored and the dataset needed for empirical definitions is thus unavailable. QPF intensity values are translated to their respective estimated return periods based on reforecast analysis (e.g., European Precipitation Index based on simulated Climatology (EPIC) [20,21]) or on intensity duration frequency (IDF) curves retrieved either from radar (e.g., Guadalhorce basin Flood Warning System (GFWS) [22], European Rainfall-Induced Hazard Assessment system (ERICHA) [23]) or rain gauge [24] observations. When the monitored catchments are assumed to share similar rainfall-runoff response behavior, a common return period value is usually applied as the threshold for all gauges covered by the system, which favors a fast interpretation of the data.

For urban environments, in which rainfall-runoff response can be highly heterogeneous in space, rainfall thresholds can be defined at neighborhood level if past FF events were properly documented. Under such circumstances, recent works have obtained acceptable results by simply performing graphical analysis of historical events [25] or by updating first-guess thresholds established from simplified hydrodynamic simulations on a hit-and-miss fashion [26]. These works illustrate the importance and applicability of high-quality disaster datasets for FF forecasting.

Since the QPF was the sole input considered by this approach, advances in precipitation forecast capabilities are considered of special benefit for rainfall comparison with surface conditions neglected (RC-SN) approaches.

2.3. Rainfall Comparison with Surface Conditions Considered (RC-SC)

The family of approaches based on rainfall comparisons with surface conditions considered (RC-SC) evaluates the raw rainfall forecasted taking into consideration the respective effective rainfall to be generated. For each location, a static flood-initiating runoff threshold (Thresh-R) value is defined. In real-time, catchment states (e.g., SSM and channel storage) are continually updated taking into consideration remotely sensed data. To consider such transient conditions, FF-generating rainfall thresholds are also dynamically updated and then compared against QPF peak values (backward comparison). The additional component, usually a hydrologic model, in the prediction chain used for tracking the estimated surface parameters increases the overall complexity of such systems. At gauged locations in which a reliable rating curve is available bank full water level values can be used as the Thresh-R [27]. For ungauged sites, Thresh-R values can be estimated from the flow frequency analysis of simulation datasets [28].

The flash flood guidance (FFG) is probably the most prominent framework of this approach. It was adopted by river forecast centers in the US in the 1970s and has been recently implemented operationally in different countries [6]. It is based on the recurrent estimation of the total raw precipitation needed to occur during specific time intervals (usually 1, 3, and 6 h) to cause flood scenarios, and the rainfall-runoff transformation is usually performed by a continuous hydrological model, be it spatially lumped flash flood guidance (LFFG) or gridded flash flood guidance (GFFG) [29,30]. Regardless of the discretization used to represent the terrain in the hydrological model, rainfall is finally represented as uniformly distributed so that a single precipitation value can be used as a threshold. The uncertainty estimation for these methods should account for both the rainfall data aggregation step [31] and the uncertainties of the own input data used [32]. Recent efforts applied to enhance the representativeness of the uncertainty associated to FFG values include the consideration of the spatial rainfall features defined through statistical analysis [33] and the adoption of Bayesian probabilistic approaches to consider the fact that the same amount of accumulated rainfall may or may not trigger floods [34].

To simplify the operational forecasting chains, promising probabilistic approaches based on Bayesian utility [35] and risk entropy [36] paradigms were presented. The probabilistic functions used to dynamically update the critical rainfall values were fitted using extensive offline hydrological model simulations assuming simplified antecedent SSM conditions.

2.4. Flow Comparison (FC)

Flow comparison (FC) approaches use QPF products as input to real-time running hydrological models so that the simulated output surface flow (expressed as surface runoff or channel discharge) is directly compared against static Thresh-R values (forward comparison). Such a direct comparison has the advantage of also providing information related to the magnitude of the upcoming event.

To enhance communication among stakeholders, Thresh-R values are usually presented in terms of the return period. Flow duration curves can be derived from grid-based statistical analysis of multiple historical simulations [37,38] or from flow quantile regionalization of gauged data [39,40].

2.5. Performance Comparison and Multi-Approach Tools

The increasing number of proposed and implemented FF forecasting systems motivated recent works based on comparative analysis to identify the most accurate approaches adopted. The critical success index (CSI) is a common metric used for assessing the efficiency of an operational system on detecting the occurrence of real FF events (hits) in studies developed over areas where a considerable number of FFs are registered. CSI also takes into consideration the observed events that were not detected (misses) and false alarms issued by:

$$CSI = \frac{\text{hits}}{\text{hits} + \text{misses} + \text{false alarms}} \quad (1)$$

in which a CSI value of 1.0 means a perfect performance, while a value of 0.0 means a total lack of skill.

A set of selected operational FFEWS is presented with their core features in Table 1. The results summarized in Table 2 from recently published comparison works illustrate how the best criterion for detecting FF scenarios depends on the target domain. Overall, the increase in complexity associated with the transition from a RC to a FC approach is justified by a significant gain in performance for systems covering large domains [38,41]. Such results motivate the inclusion of hydrological models into forecasting chains of FFEWSs under implementation [42]. However, the same pattern was not observed in studies developed over more restricted scopes [22,43]. One explanation can be that systems covering large domains may include several catchments that, despite being small, are not urbanized and present smooth relief. Such catchments are more prone to floods originated from the runoff concentration downstream of the rainfall location and are better represented by hydrologic models due to their capability to identify floods not occurring at the exact same location as the causative rainfall cell. Specific-domain systems, on the other hand, are usually implemented to cover regions known to be extremely “flashy”, be it due to the presence of urban areas and/or mountains, and the almost instantaneous process of rainfall-runoff transformation significantly reduces the role of hydrological models in the forecasting chain. However, most of the comparative works do not take into consideration RC methods based on empirical and probabilistic approaches, despite their potential to perform FF forecasts [36]. Besides the performance, another critical element to be considered is the usual lead time for FF detection associated with each approach. As reported by Lincoln [44], despite the potential for less accurately representing the actual reports of FFs, a RC-SN system using uncorrected radar rainfall estimates as the input was considered more helpful for river forecast centers operators than its FC-based counterpart fed with gauge-corrected quantitative precipitation estimations (QPE) due to the fact that the update time of the former was much shorter than the latter, thus increasing the response time of decision-makers for responsive actions.

Table 1. Summary of selected reported operational FFEWS systems sorted by criteria.

Reference	Criteria	Method System	Coverage	QPE Source	QPF Source	Resolution	Forecast Window
[20,21,45]	RC-SN	EPIC-EFAS ¹	Continental Europe	N/A	NWP ²	6 h/7 km	5 days
[23,46]	RC-SN	ERICHA-EFAS	Continental Europe	N/A	Radar extrapolation	15 min/1 km	6 h
[47]	RC-SC	FFG-BSMEFFG ³	Multinational Middle East	Satellite, radars	CP-NWP ⁴	1 h/50 km ²	6 h
[48]	RC-SC	FFG-HDRFFGS ⁵	Haiti, Dominican Republic	Satellite	CP-NWP ³	1 h/70 km ²	36 h
[38]	FC	ERIC-EFAS	Continental Europe	N/A ⁶	NWP ²	6 h/1 km	5 days
[37,49]	FC	DHM-TF-FFMP ⁷	Single large basin (US)	Radar mosaic	Radar extrapolation	1 h/4 km	1 h
[39,40,50]	FC	AIGA ⁸ -Vigicrues Flash	National (France)	Radar mosaic	N/A	15 min/1 km	6 h
[51]	FC	Flood-PROOFS ⁹	Regional (Liguria, Italy)	Satellite	Stat. down. NWP ¹⁰	30 min/1 km	3 days

¹ The European Precipitation Index based on Climatology (EPIC) was replaced operationally by the European Runoff Index based on Climatology (ERIC) in the context of the European Flood Awareness System (EFAS). ² Numerical weather prediction (NWP). ³ Black Sea and Middle East FFG system (BSMEFFG). ⁴ Convection-permitting NWP (CP-NWP). ⁵ Haiti and Dominican Republic FFG (HDRFFGS). ⁶ Soil moisture of ERIC is updated daily with NWP estimations. ⁷ Distributed Hydrologic Model-Threshold Frequency (DHM-TF) in the context of the Flash Flood Monitoring and Prediction (FFMP) program. ⁸ Geographic information adaptation for flood warning (in French: Adaptation d'Information géographique pour l'Alerte en crue—AIGA). ⁹ Flood-PRObabilistic Operational Forecasting System (Flood-PROOFS). ¹⁰ Statistical downscaling of an NWP product.

Table 2. Summary of results from selected comparative works of systems based on different flash flood identification criteria.

Reference	Criteria	Description	Best CSI *	Resolution	Coverage	Conclusion/Highlights
[52]	RC-SN	Empirical rainfall thresholds	<u>0.29</u> –0.45	30 min/Lumped	Three non-urban catchments, Italy	Simple empirically-based thresholds presented the best performance for catchments with limited datasets. Others outperformed depending on available data.
	RC-SC	Online model simulation	0.20–0.57			
	RC-SC	Bayesian utility function	0.14–0.56			
	RS-SC	Risk entropy function	0.14– <u>0.68</u>			
[41]	RC-SC	LFFG	0.19–0.34	1 h/4 km	Large monitored rural basin, US (70 stations)	Clean overperformance of the FC approach when compared to RC-SC (FFG) methods.
	RC-SC	GFFG	0.20–0.22			
	FC	DHM-TF	<u>0.32</u> – <u>0.47</u>			
[38]	RC-SN	EPIC	0.34	6 h/1 km	Continental Europe	The cost-benefit of the FC approach was positive.
	FC	ERIC	<u>0.49</u>			
[43]	RC-SN	ERICHA	N/A	10 min/1 km	Mountainous periurban region, Italy	No significant differences found in performance between the two systems.
	FC	Flood-PROOFS	N/A			
[22]	RC-SN	Rainfall IDF curves	N/A	10 min/1 km	Large poorly gauged periurban basin, Spain	Both approaches were efficient for FF forecasting, but FC is also efficient for non-FF forecasts.
	FC	Online model simulation	N/A			

* CSI values are presented in ranges when studies considered multiple scenarios. The best CSI value is underlined.

With that perspective, interactive toolsets were proposed and implemented operationally to communicate multiple metrics concurrently on clear graphic user interfaces to support decision-makers (e.g., Hydrometeorological Risks in Mediterranean and Mountainous Areas (in French: Risques Hydrométéorologiques en Territoires Montagnards et Méditerranéens—RHYTMME) [53], Flooded Locations and Simulated Hydrographs (FLASH) [54]).

3. Insights into Meteorological Contributors to Flash Floods

The problem of identifying and explaining meteorological contributing conditions to FFs causing extreme precipitation has long been explored. Extensive analysis of overall synoptic and mesoscale atmospheric patterns [9], together with the consolidation of observed and modeled datasets, motivated the development of studies focused on quantitatively identifying effective antecedent FF atmospheric descriptors to support decision-makers and response teams (the FFSA approach).

Despite overall agreement that descriptors associated to air moisture (e.g., RH, PW, T_d) and atmospheric stability (e.g., K-index, CAPE) have the high predictive potential for extreme rainfall events, and thus to pluvial FFs, there is still not a “silver bullet” combination of parameters that are widely applicable. Rather, this seems to be a problem to which solutions are either scope-, resolution- or data source-dependent. Recent works exploring observed rawinsonde data [55], atmospheric model forecasts [56,57], and reanalysis [15,58] outputs reached different optimal sets of best descriptors. These results make the use of techniques such as sensitivity analysis for feature selection (e.g., [56,57]), which is almost a mandatory step for each activity related to FF forecasting due to the increasing volume of data and candidates. However, metrics associated with PW, such as absolute [56], anomaly [55], or spatial inhomogeneity [59] values, are consistently considered powerful predictors. These findings highlight the importance of developing and enhancing methods to take into consideration such meteorological factors into forecasting chains.

4. Remote Sensing Techniques

4.1. Precipitable Water (PW)

A monitoring approach of special interest for FF forecasting due to its short update time (around 15 min) is through the analysis of the travel time delays of communication signals from dense Global Navigation Satellite System (GNSS) networks, such as the Global Positioning System (GPS).

This concept has long been explored [60] and has led to the implementation of near real-time national monitoring systems by different countries, including the US, Germany, and China [61–63]. Those systems make use of their respective national networks to complement the existing international positioning stations managed as part of the International GNSS Service. A remarkable active research field targets the development of methods to integrate additional constellations of GNSS satellites (e.g., GLONASS, BeiDou and Galileo) towards the improvement of data resolution and error reduction [64,65]. However, it has to be clarified as to how the enhancements obtained from such integration can be reflected as enhancements towards the early identification of local convective systems.

Recent lines of research explore the gains and prediction power of GPS-based PW monitoring approaches for anticipating extreme precipitation through the proposal of threshold-based techniques for issuing FF warnings [59,66] and through the use of trend analysis as a complement to radiosonde observations [67]. Despite promising results that suggest that similar experiments should be developed for further locations, there is a consensus that PW-related values alone are not sufficient to act as a pluvial FF predictor [68].

4.2. Quantitative Precipitation Estimation (QPE)

Due to the high spatiotemporal variability of precipitation events usually associated with FFs, several limitations emerge for the use of rain gauge data alone, mainly due to the low density of sensors deployed at most of the sites [69]. In this context, the use of weather radar and satellite products have

been recognized for the purpose of performing FF forecasts due to their capability to describe rainfall fields of large areas.

Recent years have witnessed the consolidation of weather radar networks with national coverage in different countries [70–73]. Those systems are totally or partially based on C- or S-band with Doppler and dual-polarization technologies, usually generating observation products with temporal resolution in the order of 5 to 10 min and spatial discretization of 0.25 to 1 km. Many operational FFEWSs with extensive coverage of ungauged basins rely on mosaic QPE products derived from those radar systems, such as the multi-sensor precipitation estimate (MPE), the high-resolution precipitation estimator (HPE) [74,75], and the precipitation composites from the Operational Program on the Exchange of Weather Radar Information (OPERA) [73]. However, some studies [76,77] indicate that radar products should present a temporal resolution of 1 min to be considered suitable for urban modeling. From that perspective, the increasing popularization of X-Band weather stations, with resolutions of up to 0.1 km/1 min, appears as the most promising advance for urban FF forecasting in the context of monitoring systems over the upcoming years [78–80]. Recently presented study cases have assessed the accuracy and positive impact of using dual-polarized X-band radar data as complements to the regional large scale networks, mainly for dense urban areas [81–83], despite the known issues associated with the high noise and susceptibility to signal attenuation that demands careful attention.

Continuous research activities have been developed to estimate the propagation of weather radar-originated uncertainties, which are considered high for both mountainous [84] and urban environments [85], on the issuing of FF warnings [32,86]. The process of merging rain gauge and radar data in real-time is a continuously researched topic, and the choice of the approach used operationally may be influenced by multiple environmental factors, such as rain gauge density, rainfall event features, proximity to the radar station and temporal resolution of the products [87], and by the level of complexity of the techniques [88]. Methods proven to enhance radar data operationally at the hourly or sub-hourly scales required for FF forecasting include mean field bias (MFB) [89], kriging with external drift (KED) [90], and Bayesian combination (BAY) [91]. However, as suggested by Ochoa-Rodriguez et al. [88], due to the ever-growing volume of heterogeneous available data, the research field would benefit from more studies exploring data-driven methods and integration of multi-source, multi-resolution datasets.

Satellite-based observations can also be considered valuable for near real-time QPE due to their usual global coverage. Rainfall rate estimations based on passive microwave (PMW) data tend to be more accurate than their infrared (IR)-based counterparts but are generated with longer latency [92] and thus may provide limited support for FF forecasting. With the continuous increase of data-availability, multi-sourced products have emerged and been improved. The Global Hydro-Estimator (GHE) from the National Oceanic and Atmospheric Administration (NOAA) is an example of a multi-constellation, IR-based operational QPE product with 15–20 min latency time and spatial resolution in the order of 4 km [93]. It is used as the input for the FFG systems installed on poorly monitored countries [6]. The deployment of new satellites equipped with sensors capable to detect a wider range of IR spectral bands, such as the undergoing replacement of the Geostationary Operational Environmental Satellites (GOES) by GOES-R series, have the potential to increase the spatial discretization of the precipitation products by up to 2 km [94]. The precipitation estimation from remotely sensed information using artificial neural networks with a cloud classification system (PERSIANN-CCS) algorithm uses a multilayer feed-forward neural network to generate QPE from IR data [95]. It was recently implemented operationally, producing rainfall products with 1 h/0.04° (~4 km) resolution and 1 h latency using PMW calibrations [96]. Despite evidencing the potential for using neural network systems towards the generation of QPE products, recent evaluation works found that such products can contain considerable underestimation of precipitation estimates and suggestion caution on their current applicability for FF forecasting [97,98].

4.3. Surface Soil Moisture (SSM)

When SSM is estimated taking into consideration precipitation as the sole water input, the neglect of other potentially relevant processes such as irrigation may result in a decreased performance of FF forecasting systems [99] into forecasting chains. This motivated the search for approaches to assimilate SSM observations [100] and to assess their gains [101] towards runoff predictions. Non-urban headwater catchments, where SSM plays a most significant role in the generation of surface runoff, are usually insufficiently equipped with in situ soil monitoring equipment capable of the needed real-time transmission. An alternative is the use of satellite data, which usually have global coverage of the top layers of soil (up to 10 cm depth) and are made freely available by their respective spatial agencies. Passive microwave-based remote sensing products have been developed and assessed during the last decades with a proper agreement with local observations [102].

The last decade witnessed the launching of a considerable number of new satellite missions capable of performing near-surface soil moisture measurements (e.g., Soil Moisture Ocean Salinity (SMOS), Soil Moisture Active Passive (SMAP), Sentinel-1). Most of the currently active products from independent satellite constellations are provided either with coarse spatial resolutions and short revisiting time (in the order of 10 km/1 day) [103–105] or the opposite (e.g., 500 m/12-days [106]), depending on the swath width of the respective sensor. For FF forecasting systems based on hydrologic models, a shorter update time was found to play a more relevant role than finer spatial discretization [107]; however, daily updates can still be considered a significant operational constraint [101,108]. In this perspective, products based on the data blending of multiple satellites missions, such as the Soil Moisture Operational Product System (SMOPS) [109], offer interesting opportunities to improve the accuracy of FF forecasts, with their potential to provide sub-daily resolution data, and their applicability for such purpose deserves to be assessed.

4.4. Drainage Network Monitoring and Controlling Systems

The data assimilation of the flow discharge observed in monitored drainage networks has the potential of reducing the uncertainties of FF forecasting systems [110,111]. Due to the potential to transport damaging objects at high velocity during extreme events, the use of non-intrusive ultrasonic or radar sensors is preferred for flash flood-prone streams over their submersible counterparts [112]. Traditionally, only the higher magnitude channels are gauged by official agencies due to the high costs associated with the acquisition and maintenance of precise equipment. Such sparse observations may not provide valuable information for small-sized neighborhoods not served by a central discharge link or for headwaters catchments prone to FFs.

Recent technological advances have led to the development of low-cost electronic systems capable of transmitting significant volumes of information through the internet making use of now widely available Wi-Fi connections, which made the deployment of several flow monitoring sensors more feasible even for channels of lower magnitude. In this perspective, the emerging concept of the Internet of Things (IoT) can be seen as an alternative to traditional supervisory control and data acquisition (SCADA) systems due to the fact that representatives of the latter tend to be isolated platforms characterized by lower levels of interoperability and scalability, while the former usually makes use of the expanding wireless availability and open communication protocols to achieve higher levels of flexibility. The IoT has been explored for the proposal and development of integrated systems capable of supporting multiple flood-related sensed data sources, with case studies presented mainly in the context of urban floods [113–115], some of them with the potential of performing autonomous decisions towards the optimization of flood-mitigating structures [115,116] in real-time.

The increased popularization of densely monitored drainage networks can thus enhance the efficiency of FF forecasting systems through the early identification of channels in overbank conditions and of sewer systems operating above their capacity, but the migration of currently implemented prototypes to effectively operational systems is yet to be assessed.

5. Precipitation Modeling and Prediction

In most cases, QPF products are the main inputs for FF forecasting chains. Methods for obtaining products with the high resolution required for FF forecasting are usually based on the downscaling of coarser numerical weather prediction (NWP) models outputs, on the temporal extrapolation of distributed remote sense observations (Figure 3), or on the integration of both approaches.

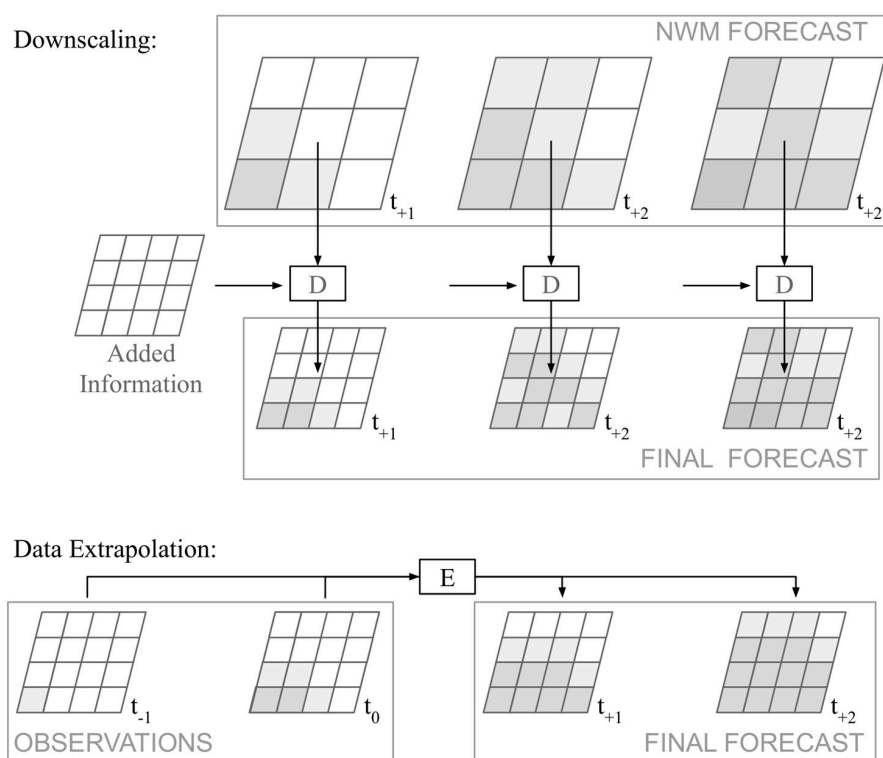


Figure 3. Schematic representation of downscaling (D) and data extrapolation (E) processes to obtain high-resolution precipitation products. The “Added Information” can be either sub-grid physics or statistical relationships.

5.1. Dynamical Downscaling

The first operational meteorological systems were limited to simulate synoptic-scale flows through hydrostatic primitive equations, in which sub-grid convective phenomena are represented indirectly using specific sets of parameters. Recent increases of overall computational power, data availability, and understanding of physical atmospheric processes allowed the consolidation of the so-called convection-permitting NWP (CP-NWP) models, which are based on hydrodynamic processes with a spatial resolution of approximately 4 km or higher, enabling the explicit representation of mesoscale events and local convection [117–120]. An illustrative selection of currently CP-NWP models in operation is summarized in Table 3.

With the experience gained with operational CP-NWP systems, multiple works were developed to assess their advantages. It has been observed that, despite increasing the overall performance when compared to their background model products, some considerations need to be taken and addressed: (1) The finer spatial scale of CP-NWP models results in higher uncertainties at the grid-scale due to spatial noise, which demands the use of ensemble systems and assessment procedures that go beyond the pixel-to-pixel comparison [121,122]; (2) CP-NWP products tend to be positively biased when compared to products from synoptic-scale models, overestimating the magnitude of extreme precipitation events [123–125], thus demanding data assimilation procedures; and (3) large-scale convective events may be better represented by synoptic-scale models than by CP-NWP [124].

The potential of overestimating extreme rainfall events was, unsurprisingly, reflected as an increase in false alarms when the products of those models were applied to FF forecasting without intermediate processing [126,127], which reasserts the need of bias correcting these products when hydrologic models are involved in the FFEWS (RC-RC or FC approaches). Due to the complex physical basis of these methods, uncertainties are usually expected to be quantified by ensemble products [128]. However, the high computational cost demanded by the higher resolution models leads to a usually reduced number of realizations being available. The work developed by Corazza et al. [129] illustrates how the Poor Man's Ensemble (PME) approach can be used to address this issue by considering ensembles composed by deterministic products originated from multiple agencies and models. The authors obtained estimated probabilities that were well correlated to observations, but a certain level of underestimation detected was associated with the fact that members of both hydrostatic and CP-NWP models were included in the ensemble. The assessment of applying the PME approach using only CP-NWP model products is promising and yet to be developed.

Table 3. Selected CP-NWP operational quantitative precipitation forecast (QPF) products sorted by spatial resolution.

Reference	Model (Product)	Agency	Coverage	Resolution	Update Cycle
[117]	WRF (HRRR)	NOAA	US	1 h/3 km	1 h
[118]	AROME (France)	Météo, France	France	1 h/1.3 km	1 h
[120]	COSMO (DE)	DWD ¹	Germany	15 min/2.8 km	3 h
[119]	HRDPS	MSC ²	Canada	1 h/2.5 km	1 h
[48]	WRF	CIMH ³	Hispaniola	1 h/4 km	6 h
[130]	ALARO (Turkey)	MGM ⁴	Turkey	1 h/4.5 km	6 h

¹ German Weather Service (DWD); ² Meteorological Services of Canada (MSC); ³ Caribbean Institute for Meteorology and Hydrology (CIMH); ⁴ Turkish State Meteorological Service (MGM).

5.2. Statistical Downscaling

One of the main advantages of using a statistical downscaling approach is the extremely low computational cost at the operational time when compared to dynamical downscaling. Statistical downscaling approaches are based on performing regression analysis between coinciding NWP-generated aerial estimations and gauge point observations. Methods successfully explored for obtaining precipitation time series with hourly temporal resolution include filtered autoregression [131], neural networks [132], and adaptable random forests [133].

Due to their statistical nature, the outputs obtained from such methods are usually directly associated with the estimation of uncertainty of physically-based models [134,135]. Flood-PRObabilistic Operational Forecasting System (Flood-PROOFS) [51] is an example of a flood forecast system that includes the downscaling model RainFARM (acronym for Rainfall Filtered Autoregressive Model) to obtain ensemble QPF of 30 min/1 km resolution from a deterministic NWP model of 7 km/3 h. The estimated uncertainties were shown to acceptably represent the errors associated with the original QPE product and illustrate the potential gains of applying statistical downscaling approaches to perform FF forecasts. However, a remarkable drawback is the recurrent need for performing statistical reanalysis every time a component of the source large-scale NWP system is changed, which limits their adoption on operational forecasting chains.

5.3. Distributed Remote Sense Data Extrapolation

Extrapolating weather radar observations of precipitation in time is similar to the computer-vision problem of predicting the next frames of a recorded video. It can be performed by extrapolating the reflectivity values observed, which has output values that later need to be converted into precipitation (radar echo extrapolation (REE)) or by directly producing QPF as output values out of the observed reflectivity, thus implicitly embedding the so-called Z-R relationship.

Motion tracking functions based on optical flow techniques have long been explored for REE. Examples of operating systems include the use of variational echo tracking [136,137] and combinations of the traditional Horn and Schunck approach with the Lucas–Kanade method [138].

The consolidation of extensive weather radar datasets allowed the development of data-driven techniques based on analog-based approaches, with promising results being obtained for locations with high orographic influence in the formation of precipitation [7,139]. Methods based on deep learning, mainly exploring the capabilities of convolutional neural networks (CNNs), have started to be explored in the last 5 years [140] and were proposed as benchmarks for precipitation nowcast methods [141]. The integration of long short-term memory (LSTM) neural network approaches with the satellite-based precipitation estimation algorithm PERSIANN-CCS was also shown to outperform optical flow-based and NWP models, mainly for capturing the patterns of convective precipitation systems [8]. However, as this is a still-emerging field, some relatively basic issues associated with the implementation of deep learning algorithms for the task of frame prediction, such as which assessment metric is the best to be used [142], are still under discussion in the community.

5.4. Multi-Model

The assessment that data extrapolation methods tend to overperform NWP models for lead times of up to 2 or 3 h (and that NWP models are more reliable for longer horizons) [143,144] motivated the exploration techniques for integrating both types of precipitation prediction products.

In the United Kingdom (UK), a dual-system approach has been adopted. By default, the stratiform-focused Nimrod [145], based on Lagrangian persistence extrapolation of radar data, is continuously executed and evaluated. When convective patterns are identified, the Generating Advanced Nowcasts for Deployment in Operational Land-based Flood forecasts (GANDOLF) [146] system, which is based on object tracking considering NWM estimated advection, is activated. Such a strategy is justified by the best individual scenario-specific performances of each model [147,148].

Recently proposed approaches with an operational adoption include Integrated Nowcasting through Comprehensive Analysis (INCA) [149–151], in which the weighting between two deterministic nowcast/forecast models is constant and dependent on the lead time. In INCA, only radar extrapolation is considered from 0 to 2 h lead time; from 3 to 6 h, both the radar extrapolation and the NWP-based products are considered, with linearly increasing of importance (weighting) of the latter with respect to the former; for 7 h onwards, only the NWP-based product is considered.

The Short-Term Ensemble Prediction System (STEPS) [152] is a probabilistic blending approach, in which uncertainties from multiple scales and sources are considered in a fractal cascade for the generation of a dynamically weighted ensemble product. The uncertainty level of each component is calculated taking into consideration the climatological analysis of the forecasted value. The method was adopted operationally in the UK and Australia in 2008 [153] and was successfully assessed for urban hydrology [154,155].

Works exploring new blending techniques are undergoing, with the proposition of approaches based on volume-correction [156] and harmony search adaptive weighting [157], for example. However, the applicability of such methods for operational FF forecasting systems requires further assessment.

6. Hydrologic-Hydraulic Modeling and Forecasting

6.1. Runoff Simulation

Mostly for non-urban, ungauged and/or data-scarce catchments, lumped models were the first to be explored and adopted operationally due to their simplicity, low level of data requirement and computational demand. Sacramento soil moisture accounting (SAC-SMA), for example, was widely used in the early versions of FFG systems in the US and is still used as part of large-domain systems with online simulations [48,54].

In the last decade, distributed rainfall-runoff and routing models were adopted operationally. Multiple river forecasting centers in the US replaced their SAC-SMA-based models with Hydrology Laboratory Research Distributed Hydrologic Model (HL-RDHM)-based counterparts. In Europe, the LISFLOOD model is used in the operational FC-based approach ERIC, which is adopted as part of EFAS [158]. Those systems operate on spatial scales in the order of 1 km to match the QPE and QPF forcings involved in the forecasting chains. However, the high number of parameters demanded by a physically-based approach may become a constraint due to the need for extensive, often unavailable, descriptive datasets or challenging calibration procedures that may result in high levels of uncertainty [159]. HL-RDHM, for example, is reported to require the calibration of 15 parameters per grid cell [160].

New models have been proposed using more hybrid conceptual-physical-based approaches to obtain more parsimonious representations of the hydrological processes. Such models intensely rely on topographic features to reduce the number of parameters used to describe the runoff and routing processes [161] and have shown to be also suitable for sub-kilometer simulations of flash flood events [162]. Operationally applied examples include the Continuum [163] and the Coupled Routing and Excess Storage (CREST) [164] models, part of the Flood-PROOFS [43] and FLASH [54] systems that require the calibration of 6 and 10 parameters per grid cell, respectively.

Arid and semi-arid regions are characterized by having more dynamic rainfall-runoff responses due to the lack of vegetation coverage and organic matter, which makes the runoff generation more dependent on the varying SSM conditions. In such regions, data assimilation of SSM can be particularly beneficial when compared to humid environments [165]. The performance of the recently presented hybrid conceptual-physical models over these specific conditions of parameter variability is yet to be assessed.

In urban areas, floods are usually initiated when the drainage systems operate above their capacity. Hydrological models can be coupled with hydraulic models so that the runoff estimated as the output by the former is used as the input flow by the latter [166]. The Storm Water Management Model (SWMM) [167], MIKE URBAN [168] and Infoworks CS are examples of established frameworks with one-dimensional (1D) components for representing hydraulic systems such as sewer networks and the presence of low-impact-development (LID) structures. The use of 1D drainage models alone are considered not suitable for representing the overflow phenomenon, but they can be used to estimate the locations of their occurrence through the identification of manholes in the overflow state, for example [169].

Hydraulic sewer models can operate at spatiotemporal resolutions in the order of centimeters/sub-minutes, which results in the need for high data availability and computational resources for online simulations. Few locations have proper and available documentation of the installed sub-surface drainage systems for an accurate model development, and the use of synthetic sewer networks derived from digital elevation models (DEMs) and structural analysis have been proposed [170] and were able to acceptably estimate the location of the underground pipes, but proper dimensioning of the diameters of the conduits is still a challenging question that may limit the applicability of such approaches for modeling extreme precipitation events [171].

Regardless of the purpose, the quantification of uncertainty associated with the model output is exceptionally being valued, which is usually achieved through the use of ensemble forecasting chains. In the context of FF forecasting, attention has been given to assess the uncertainty related to the use of precipitation nowcasts [172,173] and to scenario-specific error patterns associated with seasonality [174].

Due to the assumption that floods happen after water accumulates in the serving drainage channel, channel discharge flow modeling may not properly represent complex scenarios in which local surface ponding is observed, and flooding conditions are not necessarily associated with a channel state. Additionally, the absence of associated inundation mapping data of systems based on flow-communication only may limit the responsive steps that succeed in the forecasting phase of FFEWSs.

6.2. Flood Inundation Simulation

Accurate flood inundation maps are extremely valuable products as they have the potential to direct response efforts during emergency scenarios, particularly for dense urban areas.

Physically-based models used for the surface flow may be classified considering the spatial dimensionality supported. Two-dimensional (2D) models represent only the surface flows, thus abstracting the behavior of potentially existing drainage systems and relying on the high-quality representation of the surface through high-resolution elevation and land cover classification maps. In order to include the influence of well-described sewer networks, coupling approaches are continuously explored to integrate 1D hydraulic models. In 1D–2D modeling, the two-dimensional surface water spread is linked to the linear pipe and channel flows through connection points, such as manholes and culverts. Surface structures such as streets can also be represented as channels with linear water flows so that overland components can be simplified as 1D formulas, leading to the so-called 1D–1D coupling approaches [169]. In this context, LISFLOOD-FP [175] is a remarkable example of a widely adopted 2D model that has been assessed in urban environments at high-resolution simulations for scenarios of drainage systems overflow [176].

FF-related inundations are characterized by their high dynamicity and complexity, which demands proper representation of momentum conservation. However, solving the full 2D-forms of the Saint–Venant equation (SVE), mainly for the high spatial resolutions required in urban environments, tend to become so computationally expensive that real-time online simulations are considered unfeasible [169]. Several methods have been successfully explored to reduce the total simulation time of surface flow models with acceptable accuracy loss based on meta-modeling (or model surrogating). Physically-simplified surrogated models are based on the suppression of acceleration components of the SVE and thus are only suited for floods driven by slow flows [177,178]. The few data-driven surrogate inundation models proposed so far with adequate performance for representing spatial resolution in the order of meters were based on feed-forward neural networks and present promising results [179,180]. So far, those models have only used the simulated output maps of water depth as the training target, thus the dynamic components (such as flow velocity) associated to the flood inundation simulation have only been considered implicitly as part of the black-box training process. Their explicit consideration should be explored as a way to increase the replicability of high inertial flows, a typical feature for FFs.

The cellular automata (CA) concept explores simplified, parallelizable grid-based operations for solving field-propagation problems. In the last decade, it has been applied both for simulating sewer network flow [181] and for rapid flood inundation modeling using the Manning equation [182,183] or simplified topographic-driven water spread [184] as part of the routing process. Recent works have been developed to propose 1D–2D coupling approaches for a more realistic representation of the drainage system [185] and to improve parallelization capabilities on complex networks [186] with remarkable gains in computational time. However, the CA-based methods are still unable to replicate inundation events characterized by high inertia due to the usual neglect of momentum conservation, which can limit their applicability towards FF forecasting.

Considering that most of the physically-based inundation models assume that flood happens due to the overflows of a drainage system, which is not a necessary condition for urban environments, a new approach based on the surface water spread of instantaneous runoff generation at impervious regions was recently proposed [12]. Despite presenting promising results, the performance of the model has not been explored for scenarios of a spatial resolution higher than 50 m and its computational costs are yet to be addressed for its potential online applicability in FFEWSs.

Advances in the adoption of LiDAR technology for DEM production [187] motivated recent studies evaluating the adoption of high-resolution surface representation for urban flood inundation simulations. The positive impact of using 10 cm resolution topographic data over their respective 1 m resolution counterpart to properly represent relevant features such as curbs was assessed, but the computational cost associated with such a detailed representation may be considered a limitation

for real-time operational purposes [188,189]. The use of such a hyper-resolution dataset may require special processing so that relevant “hidden” water pathways are properly represented in the DEM. For such, structure-from-motion (SfM) techniques, which are based on photogrammetric and computer vision interpretation of overlapping photos, have showed promising results as supplementary sources of information for LiDAR [190] and for regular ground-based field surveys [191].

There is an interest in accounting for and communicating uncertainties of flood inundation maps [192]. However, the computational cost associated with the forecast runs of multiple model realizations results in unfeasible real-time operational applicability of the traditional ensemble approach. As suggested by Teng et al. [178], Gaussian processes and polynomial chaos emulation are appealing approaches to be explored in this context; however, to the best of the authors’ knowledge, no work has been developed on such a topic.

6.3. Query-Based Approaches

A family of approaches focused on making use of the high-quality simulation products obtained from full physical models without facing their expensive computational requirements in real-time is based on pre-simulating (offline) flood events caused by several different “what-if” feasible precipitation forcing scenarios. Pairs of input/output values used/obtained are stored in some sort of database schema so that, during operational time, the predicted flooding conditions (outputs) can be retrieved almost instantly from observed/forecasted conditions by a similarity search with the indexed inputs (querying) in the assumption of constant cause/consequence relationships (Figure 4). In this context, multiple combinations of methods used to represent, store, index, and query procedures have been explored.

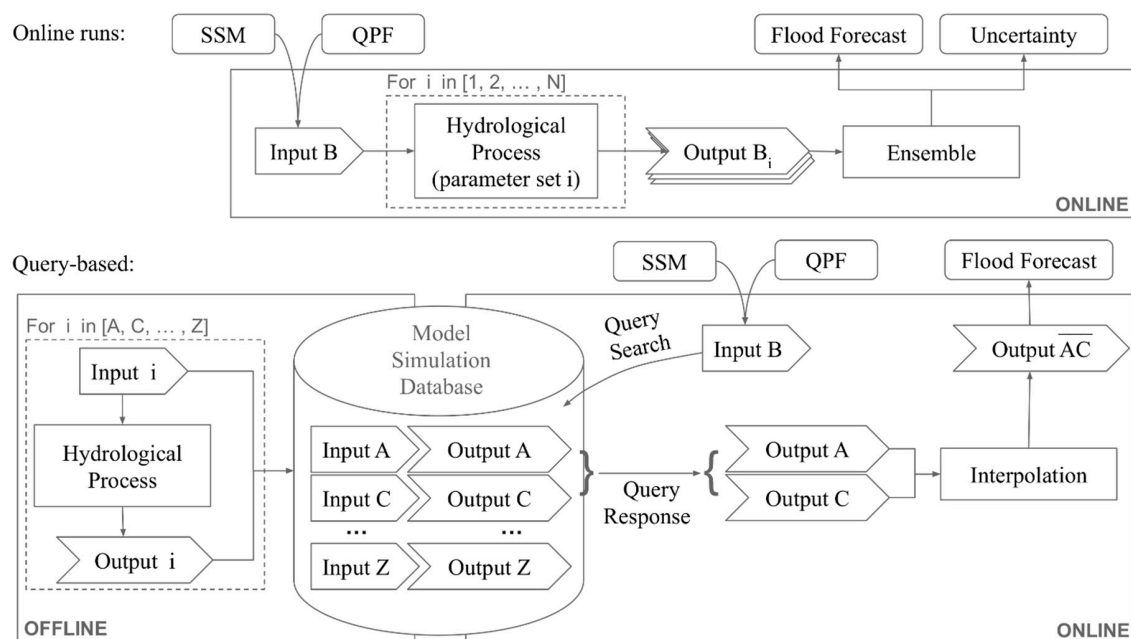


Figure 4. Comparison diagram of hypothetical online-run and query-based systems, both driven by SSM and QPF values.

One example of such an approach was presented by Song et al. [11]. The authors used the observed water depth at two locations of a channel crossing an urban area to correlate, using a 2D matrix, the Thresh-R needed to increase the water level in the systems up to a flood-triggering threshold value. The Thresh-R was then mapped backward, based on pre-simulated scenarios, into its minimum total generation precipitation intensity (P_{min}). P_{min} was finally compared with QPF values for warning issuing purposes.

Other works use a combination of self-organizing maps and recurrent neural networks to identify the most recurrent flood inundation map features simulated, thus reducing the total number of maps stored. Optimistic results were obtained for resolutions of 3 h/75 m [193] and 1 h/5 m [194] and included the modeling of a dense sewer network.

In a query-based approach, the limited number of pre-simulated scenarios does not cover all possible observable combinations of input, thus the adoption of approximation or interpolation procedures are needed. The quantification of the uncertainties derived from such an interpolation is a problem yet to be addressed.

7. Discussion and Summary

Forecasting pluvial flash floods with sufficient accuracy and lead time to support effective response actions is a challenging hydrometeorological problem that involves multiple scientific and technological fields. This work presents a non-exhaustive overview of some of the main documented operational flash flood early warning systems, of advances observed in the related topics during the last years, and of opportunities for further development.

Different criteria can be used for the prediction of a flash flood scenario. Existing operational systems may take into account meteorological patterns known to precede extreme precipitation events and apply rainfall or runoff threshold comparisons over forecasted values to identify upcoming flood events. The choice of the “best” criteria to be adopted is mainly driven by the area covered by the forecasting team and by the available resources.

For systems with national coverage in which weather radar precipitation mosaic products are available, runoff-threshold exceedance usually performs the best as the decision criterion. In this context, distributed hydrological models based on mixed conceptual-physical representations of the rainfall-runoff/routing processes are being preferred to their physically-based counterparts due to the reduced number of parameters to be calibrated. When radar coverage is insufficient, systems are being set up using satellite-derived rainfall data derived from infrared radiation measurements and using rainfall-threshold exceedance with the consideration of antecedent soil moisture conditions as warning criteria.

When a system is designed for a region or a catchment known to be dominated by flash floods, there is little evidence to justify the inclusion of a rainfall-runoff/routing model in a forecasting chain. In this context, decisions made based solely on the exceedance of a regionalized rainfall threshold may present sufficient accuracy and appropriate timely response. Raw rainfall threshold exceedance has also been shown to be a particularly efficient criterion for issuing early warnings for urban environments but, in that case, the critical values are location-specific and require proper documentation at neighborhood level of past events to be defined.

Some enhancements on deployed monitoring capabilities with the potential to enhance flash flood forecasting activities deserve to be highlighted:

- The recent expansion of global navigation satellite systems (GNSSs) allowed the development of promising multi-constellation approaches for retrieving more accurate real-time estimations of precipitable water vapor, a meteorological factor determinant on the occurrence of convective storms. However, it is not clear yet how this improvement can be reflected in our capability to anticipate precipitation events that can result in flash floods, and the research field would benefit from study cases developed in several parts of the globe to access such regional gains.
- The blending of the observations performed by recently launched satellite missions directed to monitor surface soil moisture allows products such as NOAA’s SMOPS to be produced with an update time of 6 h or less, a remarkable gain to be explored towards the estimation of antecedent soil moisture conditions when compared to the usual constraining daily revisit interval characteristic of individual missions.
- Recently presented study cases making use of dual-polarized X-band radar stations over urban areas assessed the use of such higher-resolution, short-range equipment as a positive contribution

to the already established C- and S-band wide range networks. Further deployments are seen as an essential step towards accurate flash flood monitoring in urban areas, and the use of radar extrapolation techniques for precipitation nowcasting at such a finer scale is the expected direction of further research.

- The concept of the Internet of Things, based on the reduction of the production cost of autonomous sensors capable of communicating in real-time through widely available wireless networks, has the potential to increase our deployed capability to monitor small urban channels and drainage pipes. Such dense measurement may enhance hydrological forecasts through data assimilation, but few locations have sensor networks of such type already installed and few are under study.

The main input product and the primary source of uncertainties for most of the scenarios is still the forecasted extreme precipitation products. During the last decade, we have observed the consolidation and broad operational adoption of numerical weather models with spatiotemporal resolution high enough to explicitly represent local convection. However, such higher resolution is attained with increased computational cost and spatial noise. The use of multi-model approaches, such as the Poor Man's Ensemble, applied to a set composed only by convection-permitting numeric weather models should be further considered for generating uncertainty estimations since more products of this type are expected to be made available operationally in the near future.

However, for precipitation nowcast the extrapolation of remotely-sensed rainfall fields is still considered the most accurate family of approaches. Here, novel deep learning-based techniques have been proposed as options to the traditional Lagrangian methods with promising results but, as a novel research field, some core questions are still under discussion, including which training and validating metrics should be used by the community and the size of training datasets needed for proper application of such techniques.

Flood inundation forecasts are precious products for decision-makers, but their consideration during flash floods is usually neglected due to the usually high computational time associated with the execution of traditional physically-based hydraulic models. Approaches based on data-driven surrogate modeling using machine learning, on query-based and on cellular automata have being proposed for the timely generation or retrieval of inundation maps. Despite being successfully presented in study cases with spatiotemporal resolution suitable for urban environments, further assessment is needed to validate the capability of such methods to represent the influence of high momentum flows, a characteristic of flash floods.

8. Conclusions

In the last decade, the field of flash flood forecasting has benefitted from a significant increase in overall data availability due to continuous improvements in the coverage and in spatio-temporal resolutions of monitoring and modeling systems. However, the data of such recently deployed systems is, in many cases, limited in terms of archived volume and length for proper calibration and for the adoption of data-driven modeling, a limitation that is less restrictive on older, coarser, and still well-maintained systems. The perspective presented in this work suggests that the exploration of techniques for blending multiresolution, multisource data in real-time is a major trend to benefit both the operational and research community.

The continuous deployment of early warning systems resulted in scenarios in which multiple forecasting techniques, sometimes even based on different criteria, were being executed in parallel towards the prediction of the same observed flash flood events. Such approaches facilitated the intercomparison of the performances of different methods under operational environments, and the findings suggest that systems covering large domains tend to deliver better performance when hydrological models are part of the forecast chain, while systems designed for restrict domains considered particularly flashy may present comparable efficiency by only relying on rainfall-exceedance criteria. This observation is based on a very restricted number of published comparative papers, which also illustrates the main limitation of this work, i.e., the limited number of existing FFEWSs properly

and publically documented. From that perspective, the authors highlight the importance of comparing and documenting multiple different forecasting approaches on the implementation of FFEWSs.

Author Contributions: P.C. conceived the presented idea and supervised the findings of this work. A.D.L.Z. performed data collection, investigation, critical review, and writing. All authors contributed equally in the discussion over the results and contributed to the final manuscript. All authors have read and agreed to the published version of the manuscript.

Funding: This research was supported by the Natural Science and Engineering Research Council (NSERC) of Canada, grant NSERC Canadian FloodNet (NETGP-451456).

Acknowledgments: We thank James M. Leach (McMaster University) for the valuable comments, writing assistance, and proofreading support.

Conflicts of Interest: The authors declare no conflict of interest.

Nomenclatures

AIGA	Geographic information adaptation for flood warning
BAY	Bayesian combination
BSMEFFG	Black Sea and Middle East FFG system
CA	Cellular Automata
CAPE	Convective Available Potential Energy
CNN	Convolutional Neural Network
CP-NWP	Convection Permitting Numerical Weather Prediction
CREST	Coupled Routing and Excess Storage
CSI	Critical Success Index
DEM	Digital Elevation Models
EFAS	European Flood Awareness System
EPIC	European Precipitation Index based on simulated Climatology
ERIC	European Runoff Index based on Climatology
ERICHA	European Rainfall-Induced Hazard Assessment system
FC	Flow Comparison
FF	Flash Flood
FFEWS	Flash Flood Early Warning System
FFG	Flash Flood Guidance
FFMP	Flash Flood Monitoring and Prediction
FFSA	Flash Flood Susceptibility Assessment
FLASH	Flooded Locations and Simulated Hydrographs
GFFG	Gridded Flash Flood Guidance
GFWS	Guadalorce basin Flood Warning System
GHE	Global Hydro-Estimator
GNSS	Global Navigation Satellite System
GPS	Global Position System
HDRFFGS	Haiti and Dominican Republic FFG
HPE	High-Resolution Precipitation Estimator
INCA	Integrated Nowcasting through Comprehensive Analysis
IR	Infrared
KED	Kriging with External Drift
LFFG	Lumped Flash Flood Guidance
LSTM	Long Short-Term Memory
MFB	Mean Field Bias
MPE	Multi-Sensor Precipitation Estimate
NOAA	National Oceanic and Atmospheric Administration
HL-RDHM	Hydrology Laboratory Research Distributed Hydrologic Model
IDF	Intensity Duration Frequency
IoT	Internet-of-Things
NWP	Numerical Weather Prediction

PERSIANN-CCS	Precipitation Estimation from Remotely Sensed Information using Artificial Neural Networks with a Cloud Classification System
PMW	Passive Microwave
PW	Precipitable Water
QPE	Quantitative Precipitation Estimation
QPF	Quantitative Precipitation Forecast
RC-SN	Rainfall Comparison - Surface conditions Neglected
RC-SC	Rainfall Comparison - Surface conditions Considered
REE	Radar Echo Extrapolation
RH	Relative Humidity
RHYTMME	Hydrometeorological Risks in Mediterranean and Mountainous Areas
SAC-SMA	Sacramento Soil Moisture Accounting
SCADA	Supervisory Control and Data Acquisition
SfM	Structure from Motion
SMOPS	Soil Moisture Operational Product System
SSM	Surface Soil Moisture
STEPS	Short-Term Ensemble Prediction System
SVE	Saint-Venant Equation
SWMM	Storm Water Management Model
Td	Dew Point Temperature
Thresh-R	Flood-initiating runoff threshold value
UK	United Kingdom
US	United States

References

1. Llasat, M.C.; Marcos, R.; Turco, M.; Gilabert, J.; Llasat-Botija, M. Trends in flash flood events versus convective precipitation in the Mediterranean region: The case of Catalonia. *J. Hydrol.* **2016**, *541*, 24–37. [[CrossRef](#)]
2. Yang, L.; Smith, J.A.; Wright, D.B.; Baeck, M.L.; Villarini, G.; Tian, F.; Hu, H. Urbanization and climate change: An examination of nonstationarities in urban flooding. *J. Hydrometeorol.* **2013**, *14*, 1791–1809. [[CrossRef](#)]
3. Shanableh, A.; Al-Ruzouq, R.; Yilmaz, A.G.; Siddique, M.; Merabtene, T.; Imteaz, M.A. Effects of land cover change on urban floods and rainwater harvesting: A case study in Sharjah, UAE. *Water* **2018**, *10*, 631. [[CrossRef](#)]
4. Hapuarachchi, H.A.P.; Wang, Q.J.; Pagano, T.C. A review of advances in flash flood forecasting. *Hydrol. Process.* **2011**, *25*, 2771–2784. [[CrossRef](#)]
5. National Weather Service. NWS Glossary. Available online: <https://w1.weather.gov/glossary/> (accessed on 20 January 2020).
6. Modrick, T.M.; Graham, R.; Shamir, E.; Jubach, R.; Spencer, C.R.; Sperflage, J.A.; Georgakakos, K.P. Operational flash flood warning systems with global applicability. In Proceedings of the 7th International Congress on Environmental Modelling and Software: Bold Visions for Environmental Modeling (iEMSs 2014), San Diego, CA, USA, 15–19 June 2014; pp. 694–701.
7. Panziera, L.; Germann, U.; Gabella, M.; Mandapaka, P.V. NORA-Nowcasting of Orographic Rainfall by means of analogues. *Q. J. R. Meteorol. Soc.* **2011**, *137*, 2106–2123. [[CrossRef](#)]
8. Akbari Asanjan, A.; Yang, T.; Hsu, K.; Sorooshian, S.; Lin, J.; Peng, Q. Short-term precipitation forecast based on the PERSIANN system and LSTM recurrent neural networks. *J. Geophys. Res. Atmos.* **2018**, *123*, 12543–12563. [[CrossRef](#)]
9. Maddox, R.A.; Chappell, C.F.; Hoxit, L.R. Synoptic and meso- α scale aspects of flash flood events. *Bull. Am. Meteorol. Soc.* **1979**, *60*, 155–176. [[CrossRef](#)]
10. Borga, M.; Stoffel, M.; Marchi, L.; Marra, F.; Jakob, M. Hydrogeomorphic response to extreme rainfall in headwater systems: Flash floods and debris flows. *J. Hydrol.* **2014**, *518*, 194–205. [[CrossRef](#)]
11. Song, Y.; Park, Y.; Lee, J.; Park, M.; Song, Y. Flood forecasting and warning system structures: Procedure and application to a small urban stream in South Korea. *Water* **2019**, *11*, 1571. [[CrossRef](#)]
12. Wang, X.; Kinsland, G.; Poudel, D.; Fenech, A. Urban flood prediction under heavy precipitation. *J. Hydrol.* **2019**, *577*, 123984. [[CrossRef](#)]

13. Sills, D.; Ashton, A.; Knott, S.; Boodoo, S.; Klaassen, J. A billion dollar flash flood in Toronto—Challenges for forecasting and nowcasting. In Proceedings of the 28th Conference on Severe Local Storms, Portland, OR, USA, 6–11 November 2016.
14. Doswell, C.A.; Brooks, H.E.; Maddox, R.A. Flash flood forecasting: An ingredients-based methodology. *Weather Forecast.* **1996**, *11*, 560–581. [[CrossRef](#)]
15. Jessup, S.M.; DeGaetano, A.T. A statistical comparison of the properties of flash flooding and nonflooding precipitation events in portions of New York and Pennsylvania. *Weather Forecast.* **2008**, *23*, 114–130. [[CrossRef](#)]
16. Collier, C.G.; Fox, N.I. Assessing the flooding susceptibility of river catchments to extreme rainfall in the United Kingdom. *Int. J. River Basin Manag.* **2003**, *1*, 225–235. [[CrossRef](#)]
17. George, J.J. Weather forecasting for aeronautics. *Q. J. R. Meteorol. Soc.* **1961**, *87*. [[CrossRef](#)]
18. Murray, S.J.; Smith, A.D.; Phillips, J.C. A modified flood severity assessment for enhanced decision support: Application to the Boscastle flash flood of 2004. *Weather Forecast.* **2012**, *27*, 1290–1297. [[CrossRef](#)]
19. Llorca, X.; Sánchez-Diezma, R.; Rodríguez, A.; Sancho, D.; Berenguer, M.; Sempere-Torres, D. FloodAlert: A simplified radar-based EWS for urban flood warning. In Proceedings of the 11th International Conference on Hydroinformatics, New York, NY, USA, 17–21 August 2014.
20. Alfieri, L.; Velasco, D.; Thielen, J. Flash flood detection through a multi-stage probabilistic warning system for heavy precipitation events. *Adv. Geosci.* **2011**, *29*, 69–75. [[CrossRef](#)]
21. Alfieri, L.; Thielen, J. A European precipitation index for extreme rain-storm and flash flood early warning. *Meteorol. Appl.* **2015**, *22*, 3–13. [[CrossRef](#)]
22. Versini, P.-A.; Berenguer, M.; Corral, C.; Sempere-Torres, D. An operational flood warning system for poorly gauged basins: Demonstration in the Guadalhorce basin (Spain). *Nat. Hazards* **2014**, *71*, 1355–1378. [[CrossRef](#)]
23. Park, S.; Berenguer, M.; Sempere-Torres, D. Long-term analysis of gauge-adjusted radar rainfall accumulations at European scale. *J. Hydrol.* **2019**, *573*, 768–777. [[CrossRef](#)]
24. Bezak, N.; Šraj, M.; Mikoš, M. Copula-based IDF curves and empirical rainfall thresholds for flash floods and rainfall-induced landslides. *J. Hydrol.* **2016**, *541*, 272–284. [[CrossRef](#)]
25. Papagiannaki, K.; Lagouvardos, K.; Kotroni, V.; Bezes, A. Flash flood occurrence and relation to the rainfall hazard in a highly urbanized area. *Nat. Hazards Earth Syst. Sci.* **2015**, *15*, 1859–1871. [[CrossRef](#)]
26. Jang, J.-H. An advanced method to apply multiple rainfall thresholds for urban flood warnings. *Water* **2015**, *7*, 6056–6078. [[CrossRef](#)]
27. Zhai, X.; Guo, L.; Liu, R.; Zhang, Y. Rainfall threshold determination for flash flood warning in mountainous catchments with consideration of antecedent soil moisture and rainfall pattern. *Nat. Hazards* **2018**, *94*, 605–625. [[CrossRef](#)]
28. Norbiato, D.; Borga, M.; Dinale, R. Flash flood warning in ungauged basins by use of the Flash Flood Guidance and model-based runoff thresholds. *Meteorol. Appl.* **2009**, *16*, 65–75. [[CrossRef](#)]
29. Schmidt, J.A.; Anderson, A.J.; Paul, J.H. Spatially-variable, physically-derived, flash flood guidance. In Proceedings of the 21st Conference on Hydrology, San Antonio, TX, USA, 18 January 2007.
30. Gourley, J.J.; Erlingis, J.M.; Hong, Y.; Wells, E.B. Evaluation of tools used for monitoring and forecasting flash floods in the united states. *Weather Forecast.* **2012**, *27*, 158–173. [[CrossRef](#)]
31. Ntelekos, A.A.; Georgakakos, K.P.; Krajewski, W.F. On the uncertainties of Flash Flood Guidance: Toward probabilistic forecasting of flash floods. *J. Hydrometeorol.* **2006**, *7*, 896–915. [[CrossRef](#)]
32. Villarini, G.; Krajewski, W.F.; Ntelekos, A.A.; Georgakakos, K.P.; Smith, J.A. Towards probabilistic forecasting of flash floods: The combined effects of uncertainty in radar-rainfall and flash flood guidance. *J. Hydrol.* **2010**, *394*, 275–284. [[CrossRef](#)]
33. Lee, B.J.; Kim, S. Gridded flash flood risk index coupling statistical approaches and TOPLATS land surface model for mountainous areas. *Water* **2019**, *11*, 504. [[CrossRef](#)]
34. Ghadua, Z.; Bhattacharya, B. Improving flash flood forecasting with a Bayesian probabilistic approach: A case study on the Posina Basin in Italy. *Int. J. Environ. Ecol. Eng.* **2019**, *13*, 331–337. [[CrossRef](#)]
35. Martina, M.L.V.; Todini, E.; Libralon, A. A Bayesian decision approach to rainfall thresholds based flood warning. *Hydrol. Earth Syst. Sci.* **2006**, *10*, 413–426. [[CrossRef](#)]
36. Montesarchio, V.; Ridolfi, E.; Russo, F.; Napolitano, F. Rainfall threshold definition using an entropy decision approach and radar data. *Nat. Hazards Earth Syst. Sci.* **2011**, *11*, 2061–2074. [[CrossRef](#)]

37. Reed, S.; Schaake, J.; Zhang, Z. A distributed hydrologic model and threshold frequency-based method for flash flood forecasting at ungauged locations. *J. Hydrol.* **2007**, *337*, 402–420. [[CrossRef](#)]
38. Raynaud, D.; Thielen, J.; Salamon, P.; Burek, P.; Anquetin, S.; Alfieri, L. A dynamic runoff co-efficient to improve flash flood early warning in Europe: Evaluation on the 2013 Central European floods in Germany. *Meteorol. Appl.* **2015**, *22*, 410–418. [[CrossRef](#)]
39. Javelle, P.; Demargne, J.; Defrance, D.; Pansu, J.; Arnaud, P. Evaluating flash-flood warnings at ungauged locations using post-event surveys: A case study with the AIGA warning system. *Hydrol. Sci. J.* **2014**, *59*, 1390–1402. [[CrossRef](#)]
40. Javelle, P.; Organde, D.; Demargne, J.; Saint-Martin, C.; de Saint-Aubin, C.; Garandeau, L.; Janet, B. Setting up a French national flash flood warning system for ungauged catchments based on the AIGA method. In Proceedings of the 3rd European Conference on Flood Risk Management, Lyon, France, 17–21 October 2016. [[CrossRef](#)]
41. Gourley, J.J.; Flamig, Z.L.; Hong, Y.; Howard, K.W. Evaluation of past, present and future tools for radar-based flash-flood prediction in the USA. *Hydrol. Sci. J.* **2014**, *59*, 1377–1389. [[CrossRef](#)]
42. Liu, C.; Guo, L.; Ye, L.; Zhang, S.; Zhao, Y.; Song, T. A review of advances in China’s flash flood early-warning system. *Nat. Hazards* **2018**, *92*, 619–634. [[CrossRef](#)]
43. Corral, C.; Berenguer, M.; Sempere-Torres, D.; Poletti, L.; Silvestro, F.; Rebora, N. Comparison of two early warning systems for regional flash flood hazard forecasting. *J. Hydrol.* **2019**, *572*, 603–619. [[CrossRef](#)]
44. Lincoln, S. Analysis of the 15 June 2013 isolated extreme rainfall event in Springfield, Missouri. *J. Oper. Meteorol.* **2014**, *2*, 233–245. [[CrossRef](#)]
45. Smith, P.J.; Pappenberger, F.; Wetterhall, F.; Thielen Del Pozo, J.; Krzeminski, B.; Salamon, P.; Muraro, D.; Kalas, M.; Baugh, C. On the operational implementation of the European Flood Awareness System (EFAS). In *Flood Forecasting—A Global Perspective*; Academic Press: Reading, UK, 2016; pp. 313–348, ISBN 9780128018842. [[CrossRef](#)]
46. Park, S.; Berenguer, M.; Sempere-torres, D.; Baugh, C.; Smith, P. Toward seamless high-resolution flash flood forecasting over Europe based on radar nowcasting and NWP: An evaluation with case studies. In Proceedings of the EGU General Assembly, Vienna, Austria, 23–28 April 2017.
47. Ulupinar, Y.; Akbas, A.I.; Gulsoy, E.; Celik, S.; Kose, S.; Aksoy, M. *Black Sea and Middle East Flash Flood Guidance System—User Guide*; Turkish Meteorological Service: Ankara, Turkey, 2015.
48. Shamir, E.; Georgakakos, K.P.; Spencer, C.; Modrick, T.M.; Murphy, M.J.; Jubach, R. Evaluation of real-time flash flood forecasts for Haiti during the passage of Hurricane Tomas, November 4–6, 2010. *Nat. Hazards* **2013**, *67*, 459–482. [[CrossRef](#)]
49. Cosgrove, B.A.; Clark, E.; Reed, S.; Koren, V.; Zhang, Z.; Cui, Z.; Smith, M. *Overview and Initial Evaluation of the Distributed Hydrologic Model Threshold Frequency (DHM-TF) Flash Flood Forecasting System*; US Department of Commerce: Silver Spring, MD, USA, 2012.
50. Demargne, J.; Javelle, P.; Organde, D.; Fouchier, C.; Janet, B. Enhancements of the French operational flash flood warning system, Vigicrues Flash. In Proceedings of the EGU General Assembly, Vienna, Austria, 7–12 April 2019.
51. Laiolo, P.; Gabellani, S.; Rebora, N.; Rudari, R.; Ferraris, L.; Ratto, S.; Stevenin, H.; Cauduro, M. Validation of the Flood-PROOFS probabilistic forecasting system. *Hydrol. Process.* **2014**, *28*, 3466–3481. [[CrossRef](#)]
52. Montesarchio, V.; Napolitano, F.; Rianna, M.; Ridolfi, E.; Russo, F.; Sebastianelli, S. Comparison of methodologies for flood rainfall thresholds estimation. *Nat. Hazards* **2015**, *75*, 909–934. [[CrossRef](#)]
53. Fouchier, C.; Mériaux, P.; Atger, F.; Ecrepont, S.; Liébault, F.; Bertrand, M.; Batista, D.; Azemard, P. Implementation of a real-time warning and mapping system for natural hazards triggered by rainfall in mountainous and Mediterranean areas of Southeastern France. In Proceedings of the 10th International Workshop on Precipitation in Urban Areas (UrbanRain15), Pontresina, Switzerland, 1–5 December 2015.
54. Gourley, J.J.; Flamig, Z.L.; Vergara, H.; Kirstetter, P.E.; Clark, R.A.; Argyle, E.; Arthur, A.; Martinaitis, S.; Terti, G.; Erlingis, J.M.; et al. The FLASH project—Improving the tools for flash flood monitoring and prediction across the United States. *Bull. Am. Meteorol. Soc.* **2017**, *98*, 361–372. [[CrossRef](#)]
55. Schroeder, A.; Basara, J.; Marshall Shepherd, J.; Nelson, S. Insights into atmospheric contributors to urban flash flooding across the United States using an analysis of rawinsonde data and associated calculated parameters. *J. Appl. Meteorol. Climatol.* **2016**, *55*, 313–323. [[CrossRef](#)]

56. Clark III, R.A. Machine Learning Predictions of Flash Floods. Ph.D. Thesis, University of Oklahoma, Norman, OK, USA, 2016.
57. Herman, G.R.; Schumacher, R.S. Money doesn't grow on trees, but forecasts do: Forecasting extreme precipitation with random forests. *Mon. Weather Rev.* **2018**, *146*, 1571–1600. [[CrossRef](#)]
58. Turkington, T.; Ettema, J.; Van Westen, C.J.; Breinl, K. Empirical atmospheric thresholds for debris flows and flash floods in the southern French Alps. *Nat. Hazards Earth Syst. Sci.* **2014**, *14*, 1517–1530. [[CrossRef](#)]
59. Shoji, Y. Retrieval of water vapor inhomogeneity using the Japanese nationwide GPS array and its potential for prediction of convective precipitation. *J. Meteorol. Soc. Jpn.* **2013**, *91*, 43–62. [[CrossRef](#)]
60. Bevis, M.; Businger, S.; Herring, T.A.; Rocken, C.; Anthes, R.A.; Ware, R.H. GPS meteorology: Remote sensing of atmospheric water vapor using the Global Positioning System. *J. Geophys. Res.* **1992**, *97*, 787–801. [[CrossRef](#)]
61. Ware, R.H.; Fulker, D.W.; Stein, S.A.; Anderson, D.N.; Avery, S.K.; Clark, R.D.; Droegemeier, K.K.; Kuettnner, J.P.; Minster, J.B.; Sorooshian, S. Suominet: A real-time national GPS network for atmospheric research and education. *Bull. Am. Meteorol. Soc.* **2000**, *81*, 677–694. [[CrossRef](#)]
62. Gendt, G.; Dick, G.; Reigber, C.; Tomassini, M.; Liu, Y.; Ramatschi, M. Near real time GPS water vapor monitoring for numerical weather prediction in Germany. *J. Meteorol. Soc. Jpn.* **2004**, *82*, 361–370. [[CrossRef](#)]
63. Zhang, H.; Yuan, Y.; Li, W.; Zhang, B. A real-time precipitable water vapor monitoring system using the national GNSS network of China: Method and preliminary results. *IEEE J. Sel. Top. Appl. Earth Obs. Remote Sens.* **2019**, *12*, 1587–1598. [[CrossRef](#)]
64. Li, X.; Zus, F.; Lu, C.; Dick, G.; Ning, T.; Ge, M.; Wickert, J.; Schuh, H. Retrieving of atmospheric parameters from multi-GNSS in real time: Validation with water vapor radiometer and numerical weather model. *J. Geophys. Res. Atmos.* **2015**, *120*, 7189–7204. [[CrossRef](#)]
65. Wang, J.; Wu, Z.; Semmling, M.; Zus, F.; Gerland, S.; Ramatschi, M.; Ge, M.; Wickert, J.; Schuh, H. Retrieving precipitable water vapor from shipborne multi-GNSS observations. *Geophys. Res. Lett.* **2019**, *46*, 5000–5008. [[CrossRef](#)]
66. Shi, J.; Xu, C.; Guo, J.; Gao, Y. Real-Time GPS precise point positioning-based precipitable water vapor estimation for rainfall monitoring and forecasting. *IEEE Trans. Geosci. Remote Sens.* **2015**, *53*, 3452–3459. [[CrossRef](#)]
67. Moore, A.W.; Small, I.J.; Gutman, S.I.; Bock, Y.; Dumas, J.L.; Fang, P.; Haase, J.S.; Jackson, M.E.; Laber, J.L. National Weather Service forecasters use GPS precipitable water vapor for enhanced situational awareness during the Southern California Summer monsoon. *Bull. Am. Meteorol. Soc.* **2015**, *96*, 1867–1877. [[CrossRef](#)]
68. Benevides, P.; Catalao, J.; Miranda, P.M.A. On the inclusion of GPS precipitable water vapour in the nowcasting of rainfall. *Nat. Hazards Earth Syst. Sci.* **2015**, *15*, 2605–2616. [[CrossRef](#)]
69. Mishra, A.K.; Coulibaly, P. Developments in hydrometric network design: A review. *Rev. Geophys.* **2009**, *47*. [[CrossRef](#)]
70. Saltikoff, E.; Cho, J.Y.N.; Tristant, P.; Huuskonen, A.; Allmon, L.; Cook, R.; Becker, E.; Joe, P. The threat to weather radars by wireless technology. *Bull. Am. Meteorol. Soc.* **2016**, *97*, 1159–1167. [[CrossRef](#)]
71. ECCC (Environment Climate Change Canada). Modernizing Canada's Weather-Radar Network. Available online: <https://www.canada.ca/en/environment-climate-change/services/weather-general-tools-resources/radar-overview/modernizing-network.html> (accessed on 22 January 2020).
72. Min, C.; Chen, S.; Gourley, J.J.; Chen, H.; Zhang, A.; Huang, Y.; Huang, C. Coverage of China new generation weather radar network. *Adv. Meteorol.* **2019**, *2019*, 5789358. [[CrossRef](#)]
73. Saltikoff, E.; Haase, G.; Delobbe, L.; Gaussiat, N.; Martet, M.; Idziorek, D.; Leijnse, H.; Novák, P.; Lukach, M.; Stephan, K. OPERA the radar project. *Atmosphere* **2019**, *10*, 320. [[CrossRef](#)]
74. Kitzmiller, D.; Miller, D.; Fulton, R.; Ding, F. Radar and multisensor precipitation estimation techniques in national weather service hydrologic operations. *J. Hydrol. Eng.* **2013**, *18*, 133–142. [[CrossRef](#)]
75. Willie, D.; Chen, H.; Chandrasekar, V.; Cifelli, R.; Campbell, C.; Reynolds, D.; Matrosov, S.; Zhang, Y. Evaluation of multisensor quantitative precipitation estimation in Russian river basin. *J. Hydrol. Eng.* **2017**, *22*, 1–11. [[CrossRef](#)]
76. Einfalt, T.; Arnbjerg-Nielsen, K.; Golz, C.; Jensen, N.; Quirnbach, M.; Vaes, G.; Vieux, B. Towards a roadmap for use of radar rainfall data in urban drainage. *J. Hydrol.* **2004**, *299*, 186–202. [[CrossRef](#)]
77. Thorndahl, S.; Einfalt, T.; Willems, P.; Nielsen, J.E.; ten Veldhuis, M.-C.; Arnbjerg-Nielsen, K.; Rasmussen, M.R.; Molnar, P. Weather radar rainfall data in urban hydrology. *Hydrol. Earth Syst. Sci.* **2017**, *21*, 1359–1380. [[CrossRef](#)]

78. Allegretti, M. X-Band Mini Radar for Observing and Monitoring Rainfall Events. *Atmos. Clim. Sci.* **2012**, *2*, 290–297. [[CrossRef](#)]
79. Chandrasekar, V.; Chen, H.; Philips, B. Principles of High-Resolution Radar Network for Hazard Mitigation and Disaster Management in an Urban Environment. *J. Meteorol. Soc. Jpn.* **2018**, *96A*, 119–139. [[CrossRef](#)]
80. Hirano, K.; Maki, M. Imminent nowcasting for severe rainfall using vertically integrated liquid water content derived from X-band polarimetric radar. *J. Meteorol. Soc. Jpn.* **2018**, *96A*, 201–220. [[CrossRef](#)]
81. Chen, H.; Chandrasekar, V. The quantitative precipitation estimation system for Dallas-Fort Worth (DFW) urban remote sensing network. *J. Hydrol.* **2015**, *531*, 259–271. [[CrossRef](#)]
82. Chen, H.; Lim, S.; Chandrasekar, V.; Jang, B.J. Urban hydrological applications of dual-polarization X-band radar: Case study in Korea. *J. Hydrol. Eng.* **2017**, *22*, E5016001. [[CrossRef](#)]
83. Cifelli, R.; Chandrasekar, V.; Chen, H.; Johnson, L.E. High resolution radar quantitative precipitation estimation in the San Francisco bay area: Rainfall monitoring for the urban environment. *J. Meteorol. Soc. Jpn.* **2018**, *96A*, 141–155. [[CrossRef](#)]
84. Volkmann, T.H.M.; Lyon, S.W.; Gupta, H.V.; Troch, P.A. Multicriteria design of rain gauge networks for flash flood prediction in semiarid catchments with complex terrain. *Water Resour. Res.* **2010**, *46*, W11554. [[CrossRef](#)]
85. Thorndahl, S.; Beven, K.J.; Jensen, J.B.; Schaarup-Jensen, K. Event based uncertainty assessment in urban drainage modelling, applying the GLUE methodology. *J. Hydrol.* **2008**, *357*, 421–437. [[CrossRef](#)]
86. Rafieeinassab, A.; Norouzi, A.; Kim, S.; Habibi, H.; Nazari, B.; Seo, D.J.; Lee, H.; Cosgrove, B.; Cui, Z. Toward high-resolution flash flood prediction in large urban areas—Analysis of sensitivity to spatiotemporal resolution of rainfall input and hydrologic modeling. *J. Hydrol.* **2015**, *531*, 370–388. [[CrossRef](#)]
87. McKee, J.L.; Binns, A.D. A review of gauge–radar merging methods for quantitative precipitation estimation in hydrology. *Can. Water Resour. J.* **2016**, *41*, 186–203. [[CrossRef](#)]
88. Ochoa-Rodríguez, S.; Wang, L.-P.; Willems, P.; Onof, C. A review of radar-rain gauge data merging methods and their potential for urban hydrological applications. *Water Resour. Res.* **2019**, *55*, 6356–6391. [[CrossRef](#)]
89. McKee, J.L. Evaluation of Gauge-Radar Merging Methods for Quantitative Precipitation Estimation in Hydrology: A Case Study in the Upper Thames River Basin. Master’s Thesis, The University of Western Ontario, London, ON, Canada, 2015.
90. Jewell, S.A.; Gaussiat, N. An assessment of kriging-based rain-gauge-radar merging techniques. *Q. J. R. Meteorol. Soc.* **2015**, *141*, 2300–2313. [[CrossRef](#)]
91. Wang, L.P.; Ochoa-Rodríguez, S.; Van Assel, J.; Pina, R.D.; Pessemier, M.; Kroll, S.; Willems, P.; Onof, C. Enhancement of radar rainfall estimates for urban hydrology through optical flow temporal interpolation and Bayesian gauge-based adjustment. *J. Hydrol.* **2015**, *531*, 408–426. [[CrossRef](#)]
92. Hossain, F.; Anagnostou, E.N. Assessment of current passive-microwave- and infrared-based satellite rainfall remote sensing for flood prediction. *J. Geophys. Res. D Atmos.* **2004**, *109*, 1–14. [[CrossRef](#)]
93. Scofield, R.A.; Kuligowski, R.J. Status and outlook of operational satellite precipitation algorithms for extreme-precipitation events. *Weather Forecast.* **2003**, *18*, 1037–1051. [[CrossRef](#)]
94. Kuligowski, R.J.; Li, Y.; Hao, Y.; Zhang, Y. Improvements to the GOES-R rainfall rate algorithm. *J. Hydrometeorol.* **2016**, *17*, 1693–1704. [[CrossRef](#)]
95. Hong, Y.; Hsu, K.L.; Sorooshian, S.; Gao, X. Precipitation estimation from remotely sensed imagery using an artificial neural network cloud classification system. *J. Appl. Meteorol.* **2004**, *43*, 1834–1852. [[CrossRef](#)]
96. Nguyen, P.; Ombadi, M.; Sorooshian, S.; Hsu, K.; AghaKouchak, A.; Braithwaite, D.; Ashouri, H.; Rose Thorstensen, A. The PERSIANN family of global satellite precipitation data: A review and evaluation of products. *Hydrol. Earth Syst. Sci.* **2018**, *22*, 5801–5816. [[CrossRef](#)]
97. Chen, S.; Liu, H.; You, Y.; Mullens, E.; Hu, J.; Yuan, Y.; Huang, M.; He, L.; Luo, Y.; Zeng, X.; et al. Evaluation of high-resolution precipitation estimates from satellites during July 2012 Beijing flood event using dense rain gauge observations. *PLoS ONE* **2014**, *9*, e89681. [[CrossRef](#)] [[PubMed](#)]
98. Cánovas-García, F.; García-Galiano, S.; Karbalaee, N. Validation of a global satellite rainfall product for real time monitoring of meteorological extremes. In Proceedings of the Remote Sensing for Agriculture, Ecosystems, and Hydrology XIX, SPIE, Warsaw, Poland, 2 November 2017; Volume 10421, p. 8, ISBN 9781510613065. [[CrossRef](#)]

99. Seo, D.; Lakhankar, T.; Mejia, J.; Cosgrove, B.; Khanbilvardi, R. Evaluation of operational national weather service gridded flash flood guidance over the Arkansas Red River basin. *J. Am. Water Resour. Assoc.* **2013**, *49*, 1296–1307. [[CrossRef](#)]
100. Seo, D.; Lakhankar, T.; Cosgrove, B.; Khanbilvardi, R.; Zhan, X. Applying SMOS soil moisture data into the National Weather Service (NWS)'s Research Distributed Hydrologic Model (HL-RDHM) for flash flood guidance application. *Remote Sens. Appl. Soc. Environ.* **2017**, *8*, 182–192. [[CrossRef](#)]
101. Crow, W.T.; Chen, F.; Reichle, R.H.; Liu, Q. L band microwave remote sensing and land data assimilation improve the representation of prestorm soil moisture conditions for hydrologic forecasting. *Geophys. Res. Lett.* **2017**, *44*, 5495–5503. [[CrossRef](#)] [[PubMed](#)]
102. Owe, M.; van de Griend, A.A.; Chang, A.T.C. Surface moisture and satellite microwave observations in semiarid southern Africa. *Water Resour. Res.* **1992**, *28*, 829–839. [[CrossRef](#)]
103. Bartalis, Z.; Wagner, W.; Naeimi, V.; Hasenauer, S.; Scipal, K.; Bonekamp, H.; Figa, J.; Anderson, C. Initial soil moisture retrievals from the METOP-A Advanced Scatterometer (ASCAT). *Geophys. Res. Lett.* **2007**, *34*, 5–9. [[CrossRef](#)]
104. Entekhabi, D.; Njoku, E.G.; O'Neill, P.E.; Kellogg, K.H.; Crow, W.T.; Edelstein, W.N.; Entin, J.K.; Goodman, S.D.; Jackson, T.J.; Johnson, J.; et al. The soil moisture active passive (SMAP) mission. *Proc. IEEE* **2010**, *98*, 704–716. [[CrossRef](#)]
105. Kerr, Y.H.; Waldteufel, P.; Wigneron, J.P.; Delwart, S.; Cabot, F.; Boutin, J.; Escorihuela, M.J.; Font, J.; Reul, N.; Gruhier, C.; et al. The SMOS L: New tool for monitoring key elements of the global water cycle. *Proc. IEEE* **2010**, *98*, 666–687. [[CrossRef](#)]
106. Torres, R.; Snoeij, P.; Geudtner, D.; Bibby, D.; Davidson, M.; Attema, E.; Potin, P.; Rommen, B.Ö.; Floury, N.; Brown, M.; et al. GMES Sentinel-1 mission. *Remote Sens. Environ.* **2012**, *120*, 9–24. [[CrossRef](#)]
107. Cenci, L.; Pulvirenti, L.; Boni, G.; Chini, M.; Matgen, P.; Gabellani, S.; Squicciarino, G.; Pierdicca, N. An evaluation of the potential of Sentinel 1 for improving flash flood predictions via soil moisture-data assimilation. *Adv. Geosci.* **2017**, *44*, 89–100. [[CrossRef](#)]
108. Srivastava, P.K. Satellite soil moisture: Review of theory and applications in water resources. *Water Resour. Manag.* **2017**, *31*, 3161–3176. [[CrossRef](#)]
109. Liu, J.; Zhan, X.; Hain, C.; Yin, J.; Fang, L.; Li, Z.; Zhao, L. NOAA Soil Moisture Operational Product System (SMOPS) and its validations. In Proceedings of the International Geoscience and Remote Sensing Symposium (IGARSS), Beijing, China, 10–15 July 2016; pp. 3477–3480, ISBN 9781509033324. [[CrossRef](#)]
110. Hansen, L.S.; Borup, M.; Møller, A.; Mikkelsen, P.S. Flow forecasting using deterministic updating of water levels in distributed hydrodynamic urban drainage models. *Water* **2014**, *6*, 2195–2211. [[CrossRef](#)]
111. Fava, M.C.; Mazzoleni, M.; Abe, N.; Mendionio, E.M.; Solomatine, D. An approach for urban catchment model updating. In Proceedings of the 13th International Conference on Hydroinformatics, HIC, Palermo, Italy, 01–06 July 2018; Volume 3, pp. 692–697. [[CrossRef](#)]
112. Acosta-Coll, M.; Ballester-Merelo, F.; Martinez-Peiró, M.; De la Hoz-Franco, E. Real-time early warning system design for pluvial flash floods—A review. *Sensors* **2018**, *18*, 2255. [[CrossRef](#)]
113. Yang, T.-H.; Yang, S.-C.; Kao, H.-M.; Wu, M.-C.; Hsu, H.-M. Cyber-physical-system-based smart water system to prevent flood hazards. *Smart Water* **2018**, *3*, 1–13. [[CrossRef](#)]
114. Chang, C.H.; Chung, M.K.; Yang, S.Y.; Hsu, C.T.; Wu, S.J. A case study for the application of an operational two-dimensional real-time flooding forecasting system and smart water level gauges on roads in Tainan City, Taiwan. *Water* **2018**, *10*, 574. [[CrossRef](#)]
115. Bartos, M.; Wong, B.; Kerkez, B. Open storm: A complete framework for sensing and control of urban watersheds. *Environ. Sci. Water Res. Technol.* **2018**, *4*, 346–358. [[CrossRef](#)]
116. Kerkez, B.; Gruden, C.; Lewis, M.; Montestruque, L.; Quigley, M.; Wong, B.; Bedig, A.; Kertesz, R.; Braun, T.; Cadwalader, O.; et al. Smarter stormwater systems. *Environ. Sci. Technol.* **2016**, *50*, 7267–7273. [[CrossRef](#)]
117. Powers, J.G.; Klemp, J.B.; Skamarock, W.C.; Davis, C.A.; Dudhia, J.; Gill, D.O.; Coen, J.L.; Gochis, D.J.; Ahmadov, R.; Peckham, S.E.; et al. The weather research and forecasting model: Overview, system efforts, and future directions. *Bull. Am. Meteorol. Soc.* **2017**, *98*, 1717–1737. [[CrossRef](#)]
118. Seity, Y.; Malardel, S.; Hello, G.; Bénard, P.; Bouttier, F.; Lac, C.; Masson, V. The AROME-France convective-scale operational model. *Mon. Weather Rev.* **2011**, *139*, 976–991. [[CrossRef](#)]
119. Milbrandt, J.A.; Bélair, S.; Faucher, M.; Vallée, M.; Carrera, M.L.; Glazer, A. The pan-canadian high resolution (2.5 km) deterministic prediction system. *Weather Forecast.* **2016**, *31*, 1791–1816. [[CrossRef](#)]

120. Baldauf, M.; Seifert, A.; Förstner, J.; Majewski, D.; Raschendorfer, M.; Reinhardt, T. Operational convective-scale numerical weather prediction with the COSMO model: Description and sensitivities. *Mon. Weather Rev.* **2011**, *139*, 3887–3905. [[CrossRef](#)]
121. Mittermaier, M.; Roberts, N.; Thompson, S.A. A long-term assessment of precipitation forecast skill using the Fractions Skill Score. *Meteorol. Appl.* **2013**, *20*, 176–186. [[CrossRef](#)]
122. Clark, P.; Roberts, N.; Lean, H.; Ballard, S.P.; Charlton-Perez, C. Convection-permitting models: A step-change in rainfall forecasting. *Meteorol. Appl.* **2016**, *23*, 165–181. [[CrossRef](#)]
123. Chamberlain, J.M.; Bain, C.L.; Boyd, D.F.A.; Mccourt, K.; Butcher, T.; Palmer, S. Forecasting storms over Lake Victoria using a high resolution model. *Meteorol. Appl.* **2014**, *21*, 419–430. [[CrossRef](#)]
124. Herman, G.R.; Schumacher, R.S. Extreme precipitation in models: An evaluation. *Weather Forecast.* **2016**, *31*, 1853–1879. [[CrossRef](#)]
125. Woodhams, B.J.; Birch, C.E.; Marsham, J.H.; Bain, C.L.; Roberts, N.M.; Boyd, D.F.A. What is the added value of a convection-permitting model for forecasting extreme rainfall over tropical East Africa? *Mon. Weather Rev.* **2018**, *146*, 2757–2780. [[CrossRef](#)]
126. Rogelis, M.C.; Werner, M. Streamflow forecasts from WRF precipitation for flood early warning in mountain tropical areas. *Hydrol. Earth Syst. Sci.* **2018**, *22*, 853–870. [[CrossRef](#)]
127. Snook, N.; Kong, F.; Brewster, K.A.; Xue, M.; Thomas, K.W.; Supinie, T.A.; Perfater, S.; Albright, B. Evaluation of convection-permitting precipitation forecast products using WRF, NMMB, and FV3 for the 2016–17 NOAA hydrometeorology testbed flash flood and intense rainfall experiments. *Weather Forecast.* **2019**, *34*, 781–804. [[CrossRef](#)]
128. Yussouf, N.; Knopfmeier, K.H. Application of the Warn-on-Forecast system for flash-flood-producing heavy convective rainfall events. *Q. J. R. Meteorol. Soc.* **2019**, *145*, 2385–2403. [[CrossRef](#)]
129. Corazza, M.; Sacchetti, D.; Antonelli, M.; Drofa, O. The ARPAL operational high resolution Poor Man’s Ensemble, description and validation. *Atmos. Res.* **2018**, *203*, 1–15. [[CrossRef](#)]
130. Termonia, P.; Fischer, C.; Bazile, E.; Bouyssel, F.; Brožková, R.; Bénard, P.; Bochenek, B.; Degrauwe, D.; Derková, M.; El Khatib, R.; et al. The ALADIN System and its canonical model configurations AROME CY41T1 and ALARO CY40T1. *Geosci. Model Dev.* **2018**, *11*, 257–281. [[CrossRef](#)]
131. Reborá, N.; Ferraris, L.; von Hardenberg, J.; Provenzale, A. RainFARM: Rainfall downscaling by a Filtered Autoregressive Model. *J. Hydrometeorol.* **2006**, *7*, 724–738. [[CrossRef](#)]
132. Tomassetti, B.; Verdecchia, M.; Giorgi, F. NN5: A neural network based approach for the downscaling of precipitation fields—Model description and preliminary results. *J. Hydrol.* **2009**, *367*, 14–26. [[CrossRef](#)]
133. He, X.; Chaney, N.W.; Schleiss, M.; Sheffield, J. Spatial downscaling of precipitation using adaptable random forests. *Water Resour. Res.* **2016**, *52*, 8217–8237. [[CrossRef](#)]
134. Silvestro, F.; Reborá, N. Impact of precipitation forecast uncertainties and initial soil moisture conditions on a probabilistic flood forecasting chain. *J. Hydrol.* **2014**, *519*, 1052–1067. [[CrossRef](#)]
135. Davolio, S.; Silvestro, F.; Malguzzi, P. Effects of increasing horizontal resolution in a convection-permitting model on flood forecasting: The 2011 dramatic events in Liguria, Italy. *J. Hydrometeorol.* **2015**, *16*, 1843–1856. [[CrossRef](#)]
136. Germann, U.; Zawadzki, I. Scale-dependence of the predictability of precipitation from continental radar images. Part I: Description of the methodology. *Mon. Weather Rev.* **2002**, *130*, 2859–2873. [[CrossRef](#)]
137. Yoo, C.; Lee, J.; Chang, K.; Yang, D. Sensitivity evaluation of the flash flood warning system introduced to ungauged small mountainous basins in Korea. *J. Mt. Sci.* **2019**, *16*, 971–990. [[CrossRef](#)]
138. Woo, W.C.; Wong, W.K. Operational application of optical flow techniques to radar-based rainfall nowcasting. *Atmosphere* **2017**, *8*, 48. [[CrossRef](#)]
139. Foresti, L.; Panziera, L.; Mandapaka, P.V.; Germann, U.; Seed, A. Retrieval of analogue radar images for ensemble nowcasting of orographic rainfall. *Meteorol. Appl.* **2015**, *22*, 141–155. [[CrossRef](#)]
140. Shi, X.; Chen, Z.; Wang, H. Convolutional LSTM Network: A machine learning approach for precipitation nowcasting. In Proceedings of the 28th International Conference on Neural Information Processing Systems—NIPS, Montreal, QC, Canada, 8–13 December 2015.
141. Shi, X.; Gao, Z.; Lausen, L.; Wang, H.; Yeung, D.Y.; Wong, W.K.; Woo, W.C. Deep learning for precipitation nowcasting: A benchmark and a new model. In Proceedings of the 31st International Conference on Neural Information Processing Systems—NIPS, Long Beach, CA, USA, 4–9 December 2017.

142. Tran, Q.-K.; Song, S. Computer vision in precipitation nowcasting: Applying image quality assessment metrics for training deep neural networks. *Atmosphere* **2019**, *10*, 244. [[CrossRef](#)]
143. Mandapaka, P.V.; Germann, U.; Panziera, L.; Hering, A. Can Lagrangian extrapolation of radar fields be used for precipitation nowcasting over complex alpine orography? *Weather Forecast.* **2012**, *27*, 28–49. [[CrossRef](#)]
144. Smith, P.J.; Panziera, L.; Beven, K.J. Forecasting flash floods using data-based mechanistic models and NORA radar rainfall forecasts. *Hydrol. Sci. J.* **2014**, *59*, 1403–1417. [[CrossRef](#)]
145. Golding, B.W. Nimrod: A system for generating automated very short range forecasts. *Meteorol. Appl.* **1998**, *5*, 1–16. [[CrossRef](#)]
146. Pierce, C.E.; Hardaker, P.J.; Collier, C.G.; Haggett, C.M. GANDOLF: A system for generating automated nowcasts of convective precipitation. *Meteorol. Appl.* **2000**, *7*, 341–360. [[CrossRef](#)]
147. Pierce, C.E.; Ebert, E.; Seed, A.W.; Sleigh, M.; Collier, C.G.; Fox, N.I.; Donaldson, N.; Wilson, J.W.; Roberts, R.; Mueller, C.K. The nowcasting of precipitation during Sydney 2000: An appraisal of the QPF algorithms. *Weather Forecast.* **2004**, *19*, 7–21. [[CrossRef](#)]
148. Jensen, D.G. Combining Weather Radar Nowcasts and Numerical Weather Prediction Models to Estimate Short-Term Quantitative Precipitation and Uncertainty. Ph.D. Thesis, Aalborg University, Aalborg, Denmark, 2015. [[CrossRef](#)]
149. Haiden, T.; Kann, A.; Wittmann, C.; Pistotnik, G.; Bica, B.; Gruber, C. The integrated nowcasting through comprehensive analysis (INCA) system and its validation over the Eastern Alpine region. *Weather Forecast.* **2011**, *26*, 166–183. [[CrossRef](#)]
150. Reyniers, M.; Delobbe, L. The nowcasting system INCA-BE in Belgium and its performance in different synoptic situations. In Proceedings of the 7th European Conference on radar in Meteorology and Hydrology, Toulouse, France, 25–29 June 2012.
151. Kann, A.; Pistotnik, G.; Bica, B. INCA-CE: A Central European initiative in nowcasting severe weather and its applications. *Adv. Sci. Res.* **2012**, *8*, 67–75. [[CrossRef](#)]
152. Bowler, N.E.; Pierce, C.E.; Seed, A.W. STEPS: A probabilistic precipitation forecasting scheme which merges an extrapolation nowcast with downscaled NWP. *Q. J. R. Meteorol. Soc.* **2006**, *132*, 2127–2155. [[CrossRef](#)]
153. Seed, A.W.; Pierce, C.E.; Norman, K. Formulation and evaluation of a scale decomposition-based stochastic precipitation nowcast scheme. *Water Resour. Res.* **2013**, *49*, 6624–6641. [[CrossRef](#)]
154. Liguori, S.; Rico-Ramirez, M.A. A practical approach to the assessment of probabilistic flow predictions. *Hydrol. Process.* **2013**, *27*, 18–32. [[CrossRef](#)]
155. Foresti, L.; Reyniers, M.; Seed, A.; Delobbe, L. Development and verification of a real-time stochastic precipitation nowcasting system for urban hydrology in Belgium. *Hydrol. Earth Syst. Sci.* **2016**, *20*, 505–527. [[CrossRef](#)]
156. Poletti, M.L.; Silvestro, F.; Davolio, S.; Pignone, F.; Rebor, N. Using nowcasting technique and data assimilation in a meteorological model to improve very short range hydrological forecasts. *Hydrol. Earth Syst. Sci.* **2019**, *23*, 3823–3841. [[CrossRef](#)]
157. Yoon, S.-S. Adaptive blending method of radar-based and numerical weather prediction QPFs for urban flood forecasting. *Remote Sens.* **2019**, *11*, 642. [[CrossRef](#)]
158. European Commission—Joint Research Centre. *EFAS Upgrade for the Extended Model Domain—Technical Documentation*; Publications Office of the European Union: Luxembourg, 2019; ISBN 9789279928819. [[CrossRef](#)]
159. Quintero, F.; Versini, P.A.; Baltas, E.; Berenguer, M.; Sempere-Torres, D. A radar-based flash flood forecasting for the Llobregat river basin in the Catalonia region (Spain). In Proceedings of the 35th Conference on Radar Meteorology, Pittsburgh, PA, USA, 26–30 September 2011.
160. Thorstensen, A.; Nguyen, P.; Hsu, K.; Sorooshian, S. Using densely distributed soil moisture observations for calibration of a hydrologic model. *J. Hydrometeorol.* **2016**, *17*, 571–590. [[CrossRef](#)]
161. Mantilla, R.; Gupta, V.K. A GIS numerical framework to study the process basis of scaling statistics in river networks. *IEEE Geosci. Remote Sens. Lett.* **2005**, *2*, 404–408. [[CrossRef](#)]
162. Bartsotas, N.S.; Nikolopoulos, E.I.; Anagnostou, E.N.; Solomos, S.; Kallos, G. Moving toward subkilometer modeling grid spacings: Impacts on atmospheric and hydrological simulations of extreme flash flood-inducing storms. *J. Hydrometeorol.* **2017**, *18*, 209–226. [[CrossRef](#)]

163. Silvestro, F.; Gabellani, S.; Delogu, F.; Rudari, R.; Boni, G. Exploiting remote sensing land surface temperature in distributed hydrological modelling: The example of the Continuum model. *Hydrol. Earth Syst. Sci.* **2013**, *17*, 39–62. [[CrossRef](#)]
164. Wang, J.; Yang, H.; Li, L.; Gourley, J.J.; Sadiq, K.I.; Yilmaz, K.K.; Adler, R.F.; Policelli, F.S.; Habib, S.; Irwin, D.; et al. The coupled routing and excess storage (CREST) distributed hydrological model. *Hydrol. Sci. J.* **2011**, *56*, 84–98. [[CrossRef](#)]
165. Jiang, D.; Wang, K. The role of satellite-based remote sensing in improving simulated streamflow: A review. *Water* **2019**, *11*, 1615. [[CrossRef](#)]
166. Nanía, L.S.; León, A.S.; García, M.H. Hydrologic-hydraulic model for simulating dual drainage and flooding in urban areas: Application to a catchment in the metropolitan area of Chicago. *J. Hydrol. Eng.* **2015**, *20*, 04014071. [[CrossRef](#)]
167. Rossman, L.A. *Storm Water Management Model—User’s manual version 5.1*; US EPA: Cincinnati, OH, USA, 2015.
168. Danish Hydraulic Institute (DHI). *Mike Urban Model Manager—User Guide*; DHI: Hørsholm, Denmark, 2019.
169. Henonin, J.; Russo, B.; Mark, O.; Gourbesville, P. Real-time urban flood forecasting and modelling—A state of the art. *J. Hydroinformatics* **2013**, *15*, 717–736. [[CrossRef](#)]
170. Blumensaat, F.; Wolfram, M.; Krebs, P. Sewer model development under minimum data requirements. *Environ. Earth Sci.* **2012**, *65*, 1427–1437. [[CrossRef](#)]
171. Mair, M.; Zischg, J.; Rauch, W.; Sitzenfrei, R. Where to find water pipes and sewers? On the correlation of infrastructure networks in the urban environment. *Water* **2017**, *9*, 146. [[CrossRef](#)]
172. Silvestro, F.; Rebora, N. Operational verification of a framework for the probabilistic nowcasting of river discharge in small and medium size basins. *Nat. Hazards Earth Syst. Sci.* **2012**, *12*, 763–776. [[CrossRef](#)]
173. Silvestro, F.; Rebora, N.; Cummings, G.; Ferraris, L. Experiences of dealing with flash floods using an ensemble hydrological nowcasting chain: Implications of communication, accessibility and distribution of the results. *J. Flood Risk Manag.* **2017**, *10*, 446–462. [[CrossRef](#)]
174. Quintero, F.; Sempere-Torres, D.; Berenguer, M.; Baltas, E. A scenario-incorporating analysis of the propagation of uncertainty to flash flood simulations. *J. Hydrol.* **2012**, *460–461*, 90–102. [[CrossRef](#)]
175. Bates, P.D.; De Roo, A.P.J. A simple raster-based model for flood inundation simulation. *J. Hydrol.* **2000**, *236*, 54–77. [[CrossRef](#)]
176. Fewtrell, T.J.; Bates, P.D.; Horritt, M.; Hunter, N.M. Evaluating the effect of scale in flood inundation modelling in urban environments. *Hydrol. Process.* **2008**, *22*, 5107–5118. [[CrossRef](#)]
177. Néelz, S.; Pender, G. *Benchmarking the Latest Generation of 2D Hydraulic Modelling Packages*; Environment Agency: Bristol, UK, 2013; ISBN 9781849113069.
178. Teng, J.; Jakeman, A.J.; Vaze, J.; Croke, B.F.W.; Dutta, D.; Kim, S. Flood inundation modelling: A review of methods, recent advances and uncertainty analysis. *Environ. Model. Softw.* **2017**, *90*, 201–216. [[CrossRef](#)]
179. Berkahn, S.; Fuchs, L.; Neuweiler, I. An ensemble neural network model for real-time prediction of urban floods. *J. Hydrol.* **2019**, *575*, 743–754. [[CrossRef](#)]
180. Chu, H.; Wu, W.; Wang, Q.J.; Nathan, R.; Wei, J. An ANN-based emulation modelling framework for flood inundation modelling: Application, challenges and future directions. *Environ. Model. Softw.* **2019**. [[CrossRef](#)]
181. Austin, R.J.; Chen, A.S.; Savić, D.A.; Djordjević, S. Quick and accurate Cellular Automata sewer simulator. *J. Hydroinformatics* **2014**, *16*, 1359–1374. [[CrossRef](#)]
182. Dottori, F.; Todini, E. A 2D flood inundation model based on Cellular Automata approach. In Proceedings of the XVIII International Conference on Water Resources, Barcelona, Spain, 21–24 June 2010.
183. Guidolin, M.; Chen, A.S.; Ghimire, B.; Keedwell, E.C.; Djordjević, S.; Savić, D.A. A weighted cellular automata 2D inundation model for rapid flood analysis. *Environ. Model. Softw.* **2016**, *84*, 378–394. [[CrossRef](#)]
184. Jamali, B.; Bach, P.M.; Cunningham, L.; Deletic, A. A Cellular Automata Fast Flood Evaluation (CA-ffé) Model. *Water Resour. Res.* **2019**, *55*, 4936–4953. [[CrossRef](#)]
185. Liu, L.; Liu, Y.; Wang, X.; Yu, D.; Liu, K.; Huang, H.; Hu, G. Developing an effective 2-D urban flood inundation model for city emergency management based on cellular automata. *Nat. Hazards Earth Syst. Sci.* **2015**, *15*, 381–391. [[CrossRef](#)]
186. Noh, S.J.; Lee, J.H.; Lee, S.; Kawaike, K.; Seo, D.J. Hyper-resolution 1D-2D urban flood modelling using LiDAR data and hybrid parallelization. *Environ. Model. Softw.* **2018**, *103*, 131–145. [[CrossRef](#)]

187. Chen, Z.; Gao, B.; Devereux, B. State-of-the-art: DTM generation using airborne LIDAR data. *Sensors* **2017**, *17*, 150. [[CrossRef](#)]
188. Sampson, C.C.; Fewtrell, T.J.; Duncan, A.; Shaad, K.; Horritt, M.S.; Bates, P.D. Use of terrestrial laser scanning data to drive decimetric resolution urban inundation models. *Adv. Water Resour.* **2012**, *41*, 1–17. [[CrossRef](#)]
189. de Almeida, G.A.M.; Bates, P.; Ozdemir, H. Modelling urban floods at submetre resolution: Challenges or opportunities for flood risk management? *J. Flood Risk Manag.* **2018**, *11*, S855–S865. [[CrossRef](#)]
190. Meesuk, V.; Vojinovic, Z.; Mynett, A.E.; Abdullah, A.F. Urban flood modelling combining top-view LiDAR data with ground-view SfM observations. *Adv. Water Resour.* **2015**, *75*, 105–117. [[CrossRef](#)]
191. Diakakis, M.; Andreadakis, E.; Nikolopoulos, E.I.; Spyrou, N.I.; Gogou, M.E.; Deligiannakis, G.; Katsetsiadou, N.K.; Antoniadis, Z.; Melaki, M.; Georgakopoulos, A.; et al. An integrated approach of ground and aerial observations in flash flood disaster investigations. The case of the 2017 Mandra flash flood in Greece. *Int. J. Disaster Risk Reduct.* **2019**, *33*, 290–309. [[CrossRef](#)]
192. Schumann, G.J.-P. The need for scientific rigour and accountability in flood mapping to better support disaster response. *Hydrol. Process.* **2019**, *33*, 3138–3142. [[CrossRef](#)]
193. Chang, L.-C.; Amin, M.; Yang, S.-N.; Chang, F.-J. Building ANN-based regional multi-step-ahead flood inundation forecast models. *Water* **2018**, *10*, 1283. [[CrossRef](#)]
194. Kim, H.I.; Keum, H.J.; Han, K.Y. Real-time urban inundation prediction combining hydraulic and probabilistic methods. *Water* **2019**, *11*, 293. [[CrossRef](#)]



© 2020 by the authors. Licensee MDPI, Basel, Switzerland. This article is an open access article distributed under the terms and conditions of the Creative Commons Attribution (CC BY) license (<http://creativecommons.org/licenses/by/4.0/>).